2.5. Protein integrity of HBsAg-loaded PLGA microspheres

In order to confirm the integrity of HBsAg after the microencapsulation process, the integrity of the HBsAg extracted from the PLGA microspheres was analyzed by sodium dodecyl sulfate-polyacrylamide gel electrophoresis (SDS-PAGE) and size exclusion-high performance liquid chromatography (SEC-HPLC), respectively [17,20,21]. The HBsAg-PLGA microspheres were dissolved in methylene chloride at 37 °C for 10 min. HBsAg was extracted with 0.3 ml of PBS twice and 0.4 ml of PBS once by gentle mixing and separated by centrifugation at 3000 rpm for 3 min. The aqueous layers from the three extractions were pooled and concentrated by Nanocep® (catalog: OD010C33, PALL Corp., USA). For SDS-PAGE analysis, the samples of native HBsAg and concentrated antigen extracted from the HBsAg-PLGA microspheres were loaded onto a 5% stacking gel and subjected to electrophoresis on a 15% separation gel at 200 V (Miniprotean II Electrophoresis Cell, Bio-Rad Lab., CA, USA.). The gel was stained with a 1% (w/v) silver solution. The same samples were also analyzed by SEC-HPLC using a TSK-G5000 PW_{XL} column (Tosoh Corp., Tokyo, Japan) with detection at 280 nm on a TSP-P2000 series HPLC system (Thermo Electron Corporation, MA, USA). The mobile phase was PBS (pH 6.8) delivered at a flow rate of 0.6 ml/min and the injection volume was 100 μl.

In order to confirm protein integrity of HBsAg after the microencapsulation process, the HBsAg after 72 h released from microspheres was analyzed using Western blotting [17]. About 25 mg of HBsAg-PLGA microspheres was placed in an Eppendorf tube containing 1 ml of PBS and shaken with a rotary shaker at 55 rpm and 37±0.5 °C for 72 h. Briefly, the standard and the supernatants in release test (diluted to about 0.1 μg antigen) were blotted onto a wetted nitrocellulose membrane (Hybond-c, 0.45 μm, Amersham Life Science) and blocked at room temperature for 60 min. Then, the membrane was put into the diluted solution of polyclonal anti-HBsAg antibody (purified by NCPC Gene Tech. Biotechnology Development Co., Ltd.) at 37 °C for 60 min. After 3 times of washing, the membrane was moved into the diluted horseradish peroxidase-conjugated goat anti-rabbit IgG (Beijing Zhongshan Biotechnological Corp., China) at 37 °C for 60 min. The blots were visualized with 3,3-diaminobenzidine (DAB) solution. Then, the membrane was washed by distilled water to end the reaction.

2.6. In vitro release experiments

The release of HBsAg from the PLGA microspheres was studied as follows. About 25 mg of HBsAg-PLGA microspheres was placed in an Eppendorf tube containing 1 ml of PBS and shaken with a rotary shaker at 55 rpm and 37±0.5 °C. At appropriate intervals, up to 63 days, the samples were centrifuged at 17,800 rpm for 10 min. The supernatants (700 μl) were collected and fresh buffer (700 μl) was added to control the pH, and release experiments were continued. The amount of antigen in the supernatants was determined with the BCA assay. HBsAg release profiles were generated for each microsphere formulation in terms of cumulative antigen release versus time.

2.7. Measurement of the degradation of the polymer

To investigate the degradation of the polymer of microspheres in release experiments, the change in the weight of the microspheres, the pH of the incubation solution, and the molecular weight (MW) of the polymer were measured. Blank PLGA microspheres (about 10 mg) were placed in centrifuge tubes containing 5 ml of PBS and shaken with a rotary shaker at 55 rpm and 37±0.5 °C. At specific times (0, 1, and 2 months), the samples were centrifuged at 10,000 rpm for 10 min. The pH of the supernatants was assayed. The loss of the weight of the microspheres was obtained by weighing the pellet after it was lyophilized. Then the lyophilized microspheres were dissolved in tetrahydrofuran (THF) and the MW of the polymer was determined by gel permeation chromatography (GPC) (Waters 717 plus autosampler, Waters 600 pump, Waters 2414 refractive index detector, Waters Styragel® HR4E column, Waters Corporation, Boston, USA). The detectable MW range was 50–100,000 Da, the column heater was set at 35 °C, and THF was used as the mobile phase at a flow rate of 1 ml/min.

2.8. Immunization protocol and detection of anti-HBsAg antibody

Female BALB/c mice, weighing about 20 g (6–8 weeks old), were obtained from Beijing Weitong Lihua Test Animal Co. (Beijing, China). The mice were maintained on a normal diet throughout the study. To measure anti-HBs antibody (total antibody), six groups of eight mice were injected subcutaneously (sc.) with a quantity of HBsAg, according to the following protocol: (1) three injections of 0.25 ml of HBsAg-aluminum-vaccine (10 μg/ml) at 0, 1 and 2 months, respectively, and a single injection of (2) HBsAg-PLGA50/50-COOH microspheres, (3) HBsAg-PLGA50/50 microspheres, (4) HBsAg-PLGA75/25 microspheres, (5) a mixture of HBsAg-PLGA50/50-COOH, HBsAg-PLGA50/50 and HBsAg-PLGA75/25 microspheres, and (6) 0.25 ml of 0.9% NaCl solution as a blank. The four groups of HBsAg-PLGA microspheres were weighed and dispersed in 0.25 ml of sterile 0.9% NaCl solution and the dose of HBsAg was 7.5 μg/mouse, the same as the total dose for three injections of the HBsAg-aluminum-vaccine. Blood samples were collected from the retro-orbital plexus at 1, 2, 4, 6, 8, 10, 12, 14 and 18 weeks. Sera were separated by centrifugation and stored at −20 °C until assayed.

Anti-HBs antibody was determined by quantitative ELISA using an HBsAb ELISA Kit precoated with purified HBsAg (Beijing Wantai Biological Pharmacy Enterprise Co., Ltd., China) as recommended by the manufacturer.

3. Results and discussion

3.1. Size and surface morphology of HBsAg-PLGA microspheres

The HBsAg-PLGA microspheres prepared by the "double emulsion" method in this study were basically spherical with a smooth surface as indicated by morphological examination

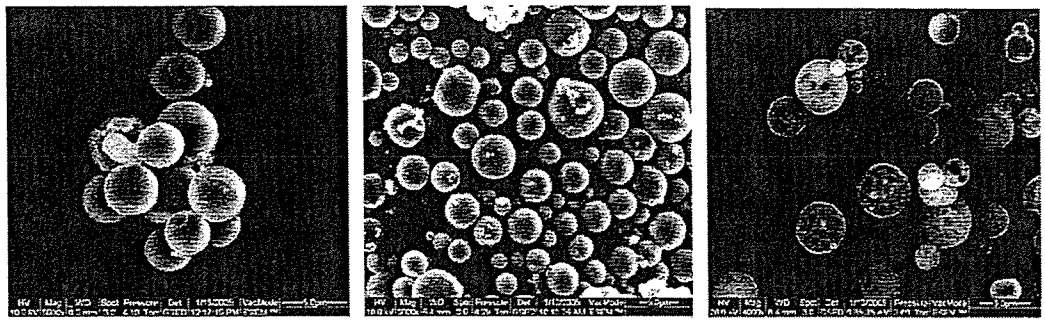

A. PLGA50/50 B. PLGA75/25 C. PLGA50/50-COOH

Fig. 1. ESEM micrographs of HBsAg-PLGA microspheres.

using ESEM (Fig. 1). Some of the HBsAg-PLGA microspheres possessed a hollow, donut-like structure and microcaves or little holes on the surface, especially the HBsAg-PLGA50/50-COOH formulation (Fig. 1C). The difference between spherical, donut-like, flattened ball-like and porous-like microspheres may be related to the species of polymer (PLGA) and the hardening and drying process. Because PLGA50/50-COOH has a lower inherent viscosity (0.22 dl/g) than the other two kinds of polymer (0.67 dl/g), the evaporation of methylene chloride during the hardening and drying of PLGA50/50-COOH may be more rapid, leading to forming more microcaves [12,22]. PLGA microspheres with microcave structures were often observed when manufactured using a spray-drying method [16,23].

Various factors including the surface morphology, particle size, polymer composition, viscosity, MW of the polymer, etc. have been shown to affect the release of antigen from microspheres, the degradation of the polymer and the immunogenicity of the antigen loaded in PLGA microspheres [24]. Size was one important factor: the larger the microspheres, the slower the release of vaccine and the longer the immunogenicity [25,26]. Table 1 lists the size determined by optical microscopy and ESEM. Although different methods of measurement of particle sizes showed different values for the three types of PLGA microspheres, the size trend of them was the same as larger order: PLGA50/50-COOH microspheres <PLGA50/50 microspheres <PLGA75/25 microspheres.

3.2. Loading efficiency of HBsAg into PLGA microspheres

The methods most commonly used to determine the protein-loading efficiency into PLGA microspheres are utilizing the BCA protein assay [12] after digestion with NaOH/SDS solution [13,15,19] or extraction with PBS from the dissolution of microspheres by organic solvents (methylene chloride, DMSO, chloroform, etc.) [19]. From the results shown in Table 1, it was concluded that the total amount of antigen encapsulated into microspheres could not be determined accurately by the method of extraction (loading efficiency determined from 18.80% to 27.17%), since a layer of whitish and cloudy protein flocculated between the interface of methylene chloride, DMSO or chloroform and aqueous layers, resulting in an underestimation of the entrapped HBsAg. The protein content of HBsAg aqueous solution obtained from extraction method (85.75%±5.17%) by BCA assay is more close to that of the digestion method (99.59%±0.98%) than that of the protein content of HBsAg-microspheres. This might be due to the protein in aqueous solution being protected by the aqueous layer all the time, and the chance to be immediately in contact with organic solvent is slight, while a portion of protein in microspheres was denatured by organic solvent when microspheres were dissolved by the organic solvent before the PBS being added. Besides, the microspheres could not be completely dissolved and antigen could not be completely extracted from the solvent layer and W/O interface. The results were in accordance with the investigation results of Gupta et al. who showed that up to 70% protein could be obtained after the solvent layer was dried and the polymer was completely digested with 6 M HCl [19]. The digestion method is a relatively accurate technique for the determination of the levels of total protein entrapped in PLGA microspheres [15].

3.3. Integrity of the antigen loaded in microspheres

The retention times of the antigen extracted from microspheres were close to those of the native antigen (13.465 min)

Table 1
Size and loading efficiency of HBsAg in PLGA microspheres

Methods of determination	Size (μm)[a]		Loading efficiency (%)	
	Optical microscopy	ESEM	Digestion (BCA)[b]	Extraction (BCA)[c]
PLGA50/50 microspheres	2.97	4.72	66.50±3.76	18.80±4.89
PLGA75/25 microspheres	4.54	6.39	76.45±4.52	27.17±2.12
PLGA50/50-COOH microspheres	1.72	3.15	73.56±1.92	22.96±5.02

[a] The size was measured by optical microscopy and Environmental Scanning Electron Microscopy (ESEM). The size data were the average of 3–5 measurements.

[b] The loading efficiency was determined by the BCA protein assay after digestion with 0.5 ml of 0.1 M NaOH/5%SDS solutions. The data represent the mean±SD (n=3). The HBsAg-PLGA microspheres were prepared using 0.65 mg HBsAg per 100 mg PLGA polymer by a double emulsion method.

[c] The loading efficiency was determined by the BCA protein assay after extraction with methylene chloride and PBS. The data represent the mean±SD (n=3).

and the purity of the extracted antigen was always above 95% from SEC-HPLC although this method has several limitations; only soluble aggregates can be measured and the size of them is overestimated (data not shown). The antigen's integrity was also examined using SDS-PAGE assays of the antigen extracted from the microspheres. Fig. 2 reveals identical bands for the native and entrapped antigen without any newly distinguishable bands, indicating there was no significant degradation or aggregation of antigens during SDS-PAGE. These results suggest that the integrity of the antigen was not significantly affected by the encapsulation procedure.

Before in vivo immunoactivity investigation, protein integrity of HBsAg after the microencapsulation process was evaluated by Western blots. Fig. 3 reveals identical blots for the native and entrapped antigen without any significant difference, suggesting that protein integrity of HBsAg before and after microencapsulation was unaltered.

3.4. Degradation of PLGA microspheres and release of antigen from the microspheres in vitro

The surface morphology of the HBsAg-PLGA microspheres incubated in PBS at 37±0.5 °C for 40 days was shown in Fig. 4. All the microspheres were in the "erosion phase," especially the PLGA50/50-COOH microspheres that were in a broken-down state. Analysis by GPC showed that the chromatograph curves of the polymer before and after encapsulation were initially fairly broad and symmetrical but gradually developed multiple peaks as the hydrolytic degradation proceeded, with many different and smaller MW components emerging. The changes of MW were summarized in Table 2. The PLGA50/50-COOH microspheres exhibited extensive erosion and breakdown at 1 and 2 months, and the degradation half-life (50% loss of molecular weight, $D_{1/2}$) was 32.7 days. In contrast, the PLGA50/50 microspheres and PLGA75/25 microspheres exhibited incomplete erosion and breakdown at 40 days (Fig. 4), and the $D_{1/2}$ was 41.5 and 116.8 days, respectively. The hydrolysis of PLGA releases lactic and glycolic acids, which may in turn lower the

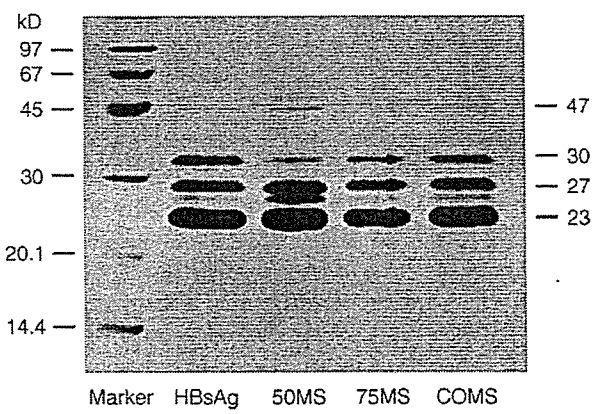

Fig. 2. SDS-PAGE of native HBsAg and entrapped HBsAg extracted from the HBsAg-PLGA50/50 microspheres (50MS), PLGA75/25 microspheres (75MS) and PLGA50/50-COOH microspheres (COMS). The MW in kDa of the peptide brands of marker after gel electrophoretic analysis is shown on the left, and the numbers on the right are those of the peptide brands of antigen.

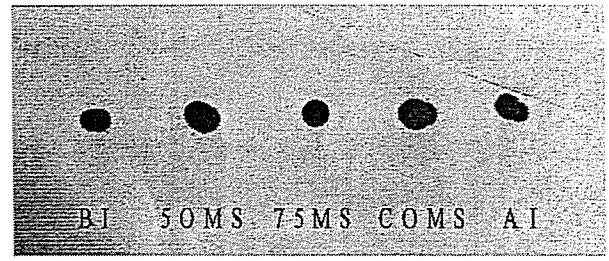

Fig. 3. Western blots of native HBsAg before (BI) and after 3 days incubation in PBS with shaking on a rotary shaker at 55 rpm and 37±0.5 °C (AI), and entrapped HBsAg released from the HBsAg-PLGA50/50 microspheres (50MS), PLGA75/25 microspheres (75MS) and PLGA50/50-COOH microspheres (COMS) incubated in PBS with shaking on a rotary shaker at 55 rpm and 37±0.5 °C after 3 days.

pH of the solution as well as the environment inside of microspheres [11]. The loss of the weight of the microspheres and the changes of pH-accompanied erosion are also given in Table 2. The PLGA50/50-COOH microspheres revealed the largest loss of weight and decrease of pH in the dissolution solution within 2 months, compared with the PLGA50/50 microspheres and PLGA75/25 microspheres. These results corresponded with the $D_{1/2}$ value of a PLGA polymer, which was related to its monomer ratio of L/G [10,27]. The results of our study indicate that in terms of the rate of degradation, the microspheres rank as follows: PLGA50/50-COOH > PLGA50/50 > PLGA75/25.

Profiles of the release of HBsAg from PLGA microspheres based on the three different polymers are shown in Fig. 5. The data are presented as the relative cumulative release of antigen from the microspheres. The PLGA50/50-COOH microspheres released HBsAg faster than the PLGA50/50 microspheres and PLGA75/25 amicrospheres, with respectively, 92.61%±1.37%, 45.2%±5.50%, and 35.35±1.73% of the antigen cumulatively released from microspheres until day-63.

The release of HBsAg seemed to correlate with the morphological changes of microspheres revealed in the ESEM images (Fig. 4), and corresponded to the decrease in MW and weight of microspheres (Table 2), suggesting that the release was controlled mainly by degradation and erosion of the polymer matrix rather than simple diffusion. That is, after microspheres emerge in the aqueous environment, with the water diffusing, the polymer swells and the antigen dissolves. As a consequence of hydrolysis of the ester bonds of polymers and formation of monomers and oligomers, microspheres become irregular in shape, develop craters on the surface, and release protein by diffusion tortuously through the water-filled polymer matrix and/or by escaping from the eroded polymer matrix [10,11,27].

The pores of the PLGA50/50-COOH microspheres might enhance the burst of initial release. When HBsAg-PLGA50/50-COOH microspheres are exposed to an aqueous environment, hydrophilic ends of the polymeric matrix are hydrated by water, the dissolved antigen can be released from the pores by osmotic pressure, and then the carboxylic ends might facilitate the autocatalytic hydrolysis of the ester bonds of the polymer and the erosion of the microspheres [11,22,27]. The PLGA50/50 and PLGA75/25 polymers with relatively high MW and viscosity

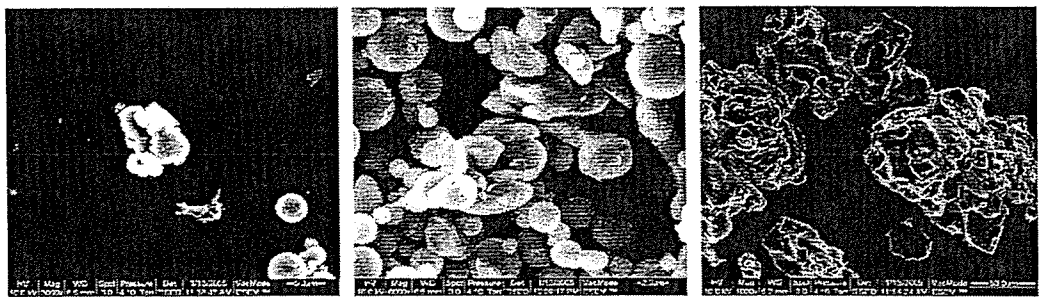

A. PLGA50/50 B. PLGA75/25 C. PLGA50/50-COOH

Fig. 4. ESEM micrographs of HBsAg-PLGA microspheres incubated in PBS with shaking on a rotary shaker at 55 rpm and 37±0.5 °C after 40 days.

may form a highly viscous polymer solution in the primary w/o emulsion and this may result in the production of compact and dense microspheres with reduced porosity. Therefore, these microspheres could minimize burst effects and slow down the release of proteins [12,22].

In addition, the size of the microspheres is also an important parameter that influences the rate at which HBsAg is released. As the particles decrease in size, the relatively high surface area per unit volume of the microspheres facilitates contact with the buffer or penetration into the microspheres and at the same time allows a faster diffusion of monomers and oligomers formed as a result of the degradation of the polymer. Then, the acidic (lactic acid and glycolic acid) monomers and oligomers further catalyze the degradation of PLGA microspheres [11,12,22,24,28].

Sánchez et al. [15] reported that PLGA microspheres with a particle size of 20–35 μm released about 50–90% of tetanus toxoid within the first day. Bittner et al. [11] reported that particles of about 18 μm with 9% loading released 60% of bovine serum albumin in an initial burst within the first day. In our study, the particle size was 1–8 μm, the antigen was loaded into microspheres rather than associated with the surface, and the loading percentage was about 0.4% (w/w), so the initial burst release of HBsAg was not observed within 24-h incubation at 37 °C in PBS. It suggested that the larger the particle size, the more antigens located on the surface of the microspheres, and then the more initial burst release. The majority of proteins were released in the first week from HBsAg-PLGA50/50-COOH microspheres, which would afford the initial burst in vivo of the mixture of three different microspheres loaded with HBsAg, corresponding to the priming immunization dose [13]. The release of antigen and the degradation of the microspheres exhibit the same trend, and the sustained release of antigen may induce an extended immunogenic response rather than an initial burst release.

3.5. Immunogenicity

The total antibody induced by the HBsAg-PLGA microspheres in vivo was analyzed by ELISA using plasma taken at different time points from immunized BALB/c mice (Fig. 6). The group that received three injections of 2.5 μg of the HBsAg-aluminum-vaccine at 0, 1 and 2 months is also shown in Fig. 6. The HBsAg-PLGA50/50-COOH microspheres produced rapidly anti-HBs antibody, which continued to fall from 6 weeks onwards compared to the HBsAg-PLGA50/50 and HBsAg-PLGA75/25 microspheres. This finding might be corresponding to the rapid release of HbsAg from PLGA50/50-COOH microspheres (Fig. 5). HBsAg-PLGA50/50-COOH microspheres might have released sufficiently during the 6 weeks and lacked of a persistent antigen stimulation to maintain the antigen concentration in the germinal center of lymphoid tissues in the latter time [29]. It suggested that HBsAg-PLGA50/50-COOH microspheres released sufficiently during the 6 weeks and lacked of an effective booster in the latter time. The fact that HBsAg-PLGA75/25 microspheres released antigen slightly slower than HBsAg-PLGA50/50 microspheres might be due to the higher MW and higher ratio of L/G of the copolymer. The

Table 2
The change of molecular weight determined by GPC, the loss of weight, pH of dissolution solution and 50% loss of MW ($D_{1/2}$) of PLGA blank microspheres incubated in PBS shaking with a rotary shaker at 55 rpm at 37±0.5 °C for 2 months

	Molecular weight of microsphere[a]			Loss of weight of microsphere (%)		pH of dissolution solution[b]		$D_{1/2}$ (day)[c]
Incubation time (month)	0	1	2	1	2	1	2	
PLGA50/50 microspheres	50,378	22,477	3699	7.63	27.69	6.96	4.45	41.5
PLGA75/25 microspheres	86,311	60,202	40,606	2.74	12.41	6.95	6.81	116.8
PLGA50/50-COOH microspheres	16,247	3724	1830	46.84	91.00	4.57	3.56	32.7

[a] The molecular weight (MW) of raw material of PLGA50/50, PLGA75/25 and PLGA50/50-COOH were 50,413, 88,148 and 18,577 Da, respectively, determined by GPC.
[b] pH of the incubation solution was 7.4 in 0 month.
[c] $D_{1/2}$:50% loss of molecular weight was calculated.

mixture of these three microspheres showed an intermediate immune response induced by the rapid release of HBsAg-PLGA50/50-COOH microspheres and the slow release of HBsAg-PLGA50/50 and HBsAg-PLGA75/25 microspheres. Until 3 months post-immunization, the antibody responses for the PLGA50/50 microspheres, PLGA75/25 microspheres and the mixture were comparable to those of the group that received three injections of the HBsAg-aluminum-vaccine ($P>0.05$), and the antibody response for the PLGA50/50-COOH microspheres was significantly lower than that for the group that received three injections of the HBsAg-aluminum-vaccine ($P<0.01$).

Shi et al. [16] reported that HBsAg-loaded PLGA microspheres 25–50 μm in size did not induce a significant immune response after a single injection with a dose of 12 μg of HBsAg, but a single injection of 3 μg of HBsAg-aluminum-vaccine plus 9 μg of HBsAg-PLGA microspheres did induce a response. Priming the mice with the HBsAg-aluminum-vaccine might lead to a greater initial response than immunization with the microspheres alone. The small particles (<10 μm) can easily be phagocytozed and transported by phagocytic APCs into the draining lymph nodes for rapid antigen release, inducing a rapid antibody response, while larger particles (>30 μm) are too large for phagocytosis, so they remain at the injection site and have the effect of continuously stimulating the immune system [26,30]. In our study, the particles were all less than 10 μm, and it is believed that the low molecular weight biodegradable polymer, formulated as small microspheres represents the major priming component of the formulation. In the present study, the antibody level induced by the mixed formulation was slightly greater than that of the HBsAg-PLGA50/50 microspheres and HBsAg-PLGA75/25 microspheres. This might be ascribed to a single injection with the mixture of three HBsAg-loaded microspheres with different particle sizes and degradation and/or release rates. The PLGA50/50-COOH microspheres with a lower MW and faster release properties like an initial priming dose generated a greater total antibody response at an early stage of the immunization, while PLGA50/50 microspheres and PLGA75/25 microspheres with a higher MW and prolonged release properties like booster doses evoked a delayed and sustained response. The results indicated that when a series of microspheres were mixed in vitro and in vivo, the release rate and the immunogenicity of vaccine-loaded PLGA microspheres might be conveniently adjusted to control the fate of the vaccine, achieving an optimal immunogenic effect.

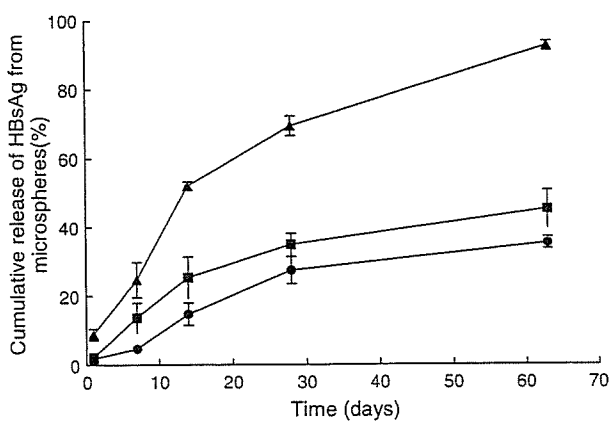

Fig. 5. Relative cumulative release of HBsAg from HBsAg-PLGA50/50-COOH microspheres (▲), HBsAg-PLGA50/50 microspheres (■) and HBsAg-PLGA75/25 microspheres (●) on different days. The HBsAg-PLGA microspheres were incubated in PBS with shaking on a rotary shaker at 55 rpm and 37± 0.5 °C.

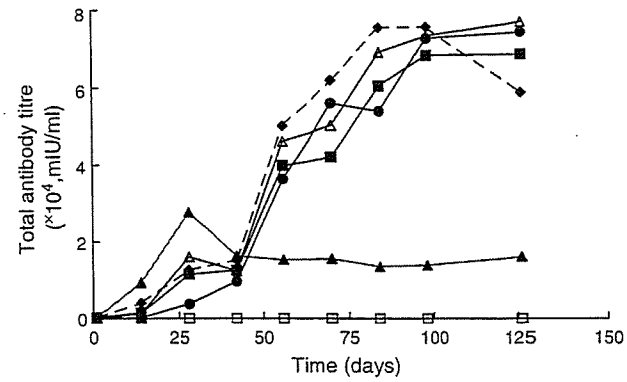

Fig. 6. Geometric mean of total antibody titer ($n=8$) obtained from BALB/c mice after immunizations with three injections of aluminum-HBsAg (2.5 μg) at 0, 1 and 2 months (–◆–), single injection of HBsAg-PLGA50/50 microspheres (–■–), PLGA75/25 microspheres (–●–), PLGA50/50-COOH microspheres (–▲–) and the three above-mentioned mixture (–△–). The blank group given 0.25 ml of 0.9% NaCl solution was expressed as (–□–). The total dose of HBsAg was 7.5 μg/mouse.

4. Conclusion

HBsAg was encapsulated in PLGA microspheres using a double emulsion method. The release of HBsAg from HBsAg-PLGA microspheres was related to the surface morphology of the microspheres, polymer composition (L/G ratio), molecular weight of the polymer (viscosity), etc. A single injection of HBsAg-PLGA microspheres had the capacity to induce a long-lasting immune response in a manner comparable to that of three injections of the HBsAg-aluminum-vaccine; the mixture of microspheres with different release rates in particular induced a strong anti-HBsAg antibody response. The rapid-release PLGA50/50-COOH microspheres were used as a priming dose, and the prolonged-release PLGA50/50 microspheres and PLGA75/25 microspheres were used as an "autobooster dose." Adjustment of the kinetics of antigen release and degradation of polymer could control and manipulate an optimal immune response.

Acknowledgements

We would like to thank Rui Hui Guo, Xi Ming Chen, Xue Qiang Yao, Yong Lu and Jie Geng in NCPC Gene Tech Biotechnology Development Co., Ltd. for offering HBsAg aqueous solution, HBsAg-aluminum-vaccines and administrative assistance, Wu Xiao Ding, Hui Li Ma, Li Yang, and Jing Shi in Department of Pharmaceutics, School of Pharmaceutical Sciences, Peking University and Wei Ting Zhang, Li Fang Guo, Hui Xin Hou, Jin Li Chen, Xin Yu Fan, and Li Xia Zheng of NCPC Gene Tech Biotechnology Development Co., Ltd. for

technical assistance, and Han Cheng Yuan and Hao Liang Gu of Waters China Ltd. for their enormous help with GPC studies.

References

[1] S. Thoelen, N.D. Clercq, N. Tornieporth, A prophylactic hepatitis B vaccine with a novel adjuvant system, Vaccine 19 (2001) 2400–2403.
[2] X.C. Guo, Z.J. Yi, J.P. Bi, The status in China of the development of recombinant hepatitis B vaccine expressed by Chinese Hamster Ovary (CHO), Dis. Monit. 14 (4) (1999) 238–239.
[3] D. Shouval, Hepatitis B vaccines, J. Hepatol. 39 (2003) S70–S76.
[4] Q.L. Dai, M.J. Zhang, Discussion about the prevention of hepatitis B and gene technological hepatitis B vaccines, China Pharm. 12 (2) (2003) 44.
[5] R.K. Gupta, G.R. Siber, Adjuvants for human vaccines—current status, problems and future prospects, Vaccine 13 (14) (1995) 1263–1276.
[6] C.J. Clements, E. Griffiths, The global impact of vaccines containing aluminium adjuvants, Vaccine 20 (2002) S24–S33.
[7] S. Wang, X. Liu, M.J. Caulfield, Adjuvant synergy in the response to hepatitis B vaccines, Vaccine 21 (2003) 4297–4306.
[8] Y. Men, C. Thomasin, H.P. Merkle, B. Gander, G. Corradin, A single administration of tetanus toxoid in biodegradable microspheres elicits T cell and antibody responses similar or superior to those obtained with aluminium hydroxide, Vaccine 13 (7) (1995) 683–689.
[9] P. Johansen, B. Gander, H.P. Merkle, D. Sesardic, Ambiguities in the preclinical quality assessment of microparticulate vaccines, Trends Biotechnol. 18 (2000) 203–210.
[10] S. Cohen, L. Chen, Ron N. Apte, Controlled release of peptides and proteins from biodegradable polyester microspheres: an approach for treating infectious diseases and malignancies, React. Polym. 25 (1995) 177–187.
[11] B. Bittner, C. Witt, K. Mäder, T. Kissel, Degradation and protein release properties of microspheres prepared from biodegradable poly (lactide-co-glycolide) and ABA triblock copolymers: influence of buffer media on polymer erosion and bovine serum albumin release, J. Control. Release 60 (1999) 297–309.
[12] H. Sah, R. Toddywala, Y.W. Chien, Continuous release of proteins from biodegradable microcapsules and in vivo evaluation of their potential as a vaccine adjuvant, J. Control. Release 35 (1995) 137–144.
[13] M. Singh, X.M. Li, J.P. McGee, T. Zamb, W. Koff, C.Y. Wang, D.T. O'Hagan, Controlled release microparticles as a single dose hepatitis B vaccine: evaluation of immunogenicity in mice, Vaccine 15 (5) (1997) 475–481.
[14] A.B. Sasiak, B. Bolgiano, D.T. Crane, D.J. Hockley, M.J. Corbel, D. Sesardic, Comparison of in vitro and in vivo methods to study stability of PLGA microencapsulated tetanus toxoid vaccines, Vaccine 19 (2001) 694–705.
[15] A. Sánchez, B. Villamayor, Y. Guo, J. Melver, M.J. Alonso, Formulation strategies for the stabilization of tetanus toxoid in poly (lactide-co-glicolide) microspheres, Int. J. Pharm. 185 (1999) 255–266.
[16] L. Shi, M.J. Caulfield, R.T. Chem, R.A. Wilson, G. Sanyal, D.B. Volkin, Pharmaceutical and immunological evaluation of a single-shot hepatitis B vaccine formulated with PLGA microspheres, J. Pharm. Sci. 91 (2002) 1020–1035.
[17] K.S. Jaganathan, P. Singh, D. Prabakaran, Development of a single-dose stabilized poly (D,L-lactide-co-glycolide) miceospheres-based vaccine against hepatitis B, J. Pharm. Pharmacol. 56 (2004) 1243–1250.
[18] T. Kissel, et al., in: B. Gander, H.P. Merkle, G. Corradin (Eds.), Antigen Delivery Systems: Immunological and Technological Issues, vol. 8, Harwood Academic Publishers, 1997, p. 184.
[19] R.K. Gupta, A.-C. Chang, P. Griffin, R. Rivera, Y.-Y. Guo, G.R. Siber, Determination of protein loading in biodegradable polymer microspheres containing tetanus toxoid, Vaccine 15 (6/7) (1997) 672–678.
[20] J. Wang, K.M. Hua, C.-H. Wang, Stabilization and encapsulation of human immunoglobulin G into biodegradable microspheres, J. Control. Interface Sci. 271 (2004) 92–101.
[21] N. Kofler, C. Ruedl, J. Klima, H. Recheis, G. Böck, G. Wick, H. Wolf, Preparation and characterization of poly (lactide-co-glicolide) microspheres with entrapped pneumotropic bacterial antigens, J. Immunol. Methods 192 (1996) 25–35.
[22] R. Ghaderi, C. Aturesson, J. Carlfors, Effect of preparative parameters on the characteristics of poly (D,L-lactide-co-glycolide) miceospheres made by the double emulsion method, Int. J. Pharm. 141 (1996) 205–216.
[23] L. Mu, S.S. Feng, Fabrication, characterization and in vitro release of paclitaxel (Taxol®) loaded poly (lactic-co-glycolic acid) microspheres prepared by spray drying technique with lipid/cholesterol emulsifiers, J. Control. Release 76 (2001) 239–254.
[24] J. Panyam, M.M. Dali, S.K. Sahoo, W. Ma, S.S. Chakravarthi, G.L. Amidon, R.J. Levy, Polymer degradation and in vitro release of a model protein from poly (D, L-lactide-co-glycolide) nano- and microparticles, J. Control. Release 92 (2003) 173–187.
[25] Y. Men, et al., in: B. Gander, H.P. Merkle, G. Corradin (Eds.), Antigen Delivery Systems: Immunological and Technological Issues, vol. 8, Harwood Academic Publishers, Australia, 1997, pp. 191–205.
[26] R.K. Gupta, J. Alroy, M.J. Alonso, R. Langer, G.R. Siber, Chronic local tissue reactions, long term immunogenicity and immunologic priming of mice guinea pigs to tetanus toxoid encapsulated in biodegradable polymer microspheres composed of poly lactide-co-glycolide polymers, Vaccine 15 (16) (1997) 1716–1723.
[27] J.M. Anderson, M.S. Shive, Biodegradation and biocompatibility of PLA and PLGA microspheres, Adv. Drug Deliv. Rev. 28 (1997) 5–24.
[28] J.L. Cleland, in: M.F. Powell, M.J. Wewman (Eds.), Vaccine Design: The Subunit and Adjuvant Approach, Plenum Press, New York, 1995, pp. 447–449.
[29] G.Y. Zhou, et al., in: G.Y. Zhou (Ed.), Principles of Immunology, Shanghai Science Technology Literature Press, Shanghai, 2003, pp. 12–14.
[30] J.H. Eldridge, J.K. Staas, J.A. Meulbroek, T.R. Tice, R.M. Gilley, Biodegradable and biocompatible poly (lactide-co-glicolide) microspheres as an adjuvant for staphylococcal enterotoxin B toxoid which enhances the level of toxin-neutralising antibodies, Infect. Immun. 59 (1991) 2978–2986.

Available online at www.sciencedirect.com
SCIENCE DIRECT
ELSEVIER
International Journal of Pharmaceutics 316 (2006) 109–116
INTERNATIONAL JOURNAL OF PHARMACEUTICS
www.elsevier.com/locate/ijpharm

Design, synthesis and gene delivery efficiency of novel oligo-arginine-linked PEG-lipids: Effect of oligo-arginine length

Masahiko Furuhata [a], Hiroko Kawakami [b], Kazunori Toma [b], Yoshiyuki Hattori [a], Yoshie Maitani [a,*]

[a] *Institute of Medicinal Chemistry, Hoshi University, Ebara 2-4-41, Shinagawa-ku, Tokyo 142-8501, Japan*
[b] *The Noguchi Institute, Kaga 1-8-1, Itabashi-ku, Tokyo 173-0003, Japan*

Received 17 September 2005; received in revised form 2 February 2006; accepted 24 February 2006
Available online 4 April 2006

Abstract

The design, synthesis, and evaluation of in vitro gene delivery efficacy of a novel series of oligo-Arg-lipid conjugates are described. 3,5-Bis(dodecyloxy)benzamide (BDB) was employed as the lipid component, and a poly(ethylene glycol) (PEG) spacer was introduced between the C-terminal of oligo-Arg and the amide group of BDB. Four derivatives with various oligo-Arg lengths (ArgN-PEG-BDB; $N=4$, 6, 8, 10: the number of arginine residues) were prepared, and the effect of oligo-Arg length on the gene transfection was investigated in HeLa cells. Transfection efficiency increased as the number of arginine residues increased. Arg10-PEG-BDB showed the highest transfection efficiency, without severe toxicity to cells. These findings well corresponded to the cellular association of the Arg-PEG-BDB/DNA complex determined by flow cytometry. Even in the presence of serum, Arg10-PEG-BDB achieved appreciable cellular association and attained high gene expression. Thus, Arg10-PEG-BDB is potentially a simple and useful gene delivery tool, because one need only to mix it with plasmid DNA and apply the complexes to the cells even in a serum-containing medium.

Keywords: Cell penetrating peptides; Oligo-arginine; Gene delivery

1. Introduction

Cationic lipid-based gene transfection constitutes one of the most promising alternatives to the use of viral vectors (Felgner et al., 1987; Song et al., 1998; Cotten et al., 1990; Kircheis et al., 1999; Brown et al., 2000). However, the low-level transfection efficiency compared with viral vectors is considered a major limitation in the application to gene therapy. The poor efficiency is supposed to arise from the endocytic route of internalization of cationic lipids complexed with DNA. Therefore, novel and more efficient synthetic vectors, hopefully with a different cell internalization mechanism, are desired.

Recently, a cellular internalization method using short peptides derived from protein-transduction domains has attracted much attention. Several cell penetrating peptides (CPPs), such as HIV-1 Tat fragments, less than 30 amino acid residues in length, have the capability of crossing a plasma membrane (Derossi et al., 1994; Vives et al., 1997; Oehlke et al., 1998; Pooga et al., 1998; Futaki et al., 2001a; Morris et al., 2001). In addition, they can deliver their associated molecules into cells. The Tat peptide has been reported to be capable of delivering β-galactosidase (120 kDa) to various organs when administered intraperitoneally to mice (Schwarze et al., 1999), and even nanoparticles (Lewin et al., 2000) and liposomes (Torchilin et al., 2001) can be delivered into cells. Although the mechanism of cell internalization is still incompletely understood, it is reported to be different from that of liposome vectors, which are internalized via an energy-independent pathway (Derossi et al., 1994; Vives et al., 1997). Oligo-arginine (Arg) conjugates were demonstrated to have characteristics similar to CPPs in cell translocation (Mitchell et al., 2000; Wender et al., 2000; Futaki et al., 2001a).

Although investigations delineating the influence of Arg length on the transfection efficiency and uptake of oligo-Args have been reported (Mitchell et al., 2000; Wender et al., 2000; Futaki et al., 2001a,b), there is no report about oligo-Arg-linked poly(ethylene glycol) (PEG) lipids alone as a gene vector. The

* Corresponding author. Tel.: +81 3 5498 5048; fax: +81 3 5498 5048.
E-mail address: yoshie@hoshi.ac.jp (Y. Maitani).

0378-5173/$ – see front matter © 2006 Elsevier B.V. All rights reserved.
doi:10.1016/j.ijpharm.2006.02.041

aim of this study was to design and synthesize simple and effective vectors for use in gene delivery. Oligo-Arg-linked PEG-lipids might have the ability to electrostatically stabilize naked DNA and mediate gene transfection through a non-endocytotic pathway.

In the present study, we synthesized oligo-Arg-lipids of quite different structure from a reported one (Futaki et al., 2001b), employing 3,5-bis (dodecyloxy)benzamide (BDB) as the lipid component, and introducing a PEG spacer between the C-terminal of oligo-Arg and the amide group of BDB (oligo-Arg-PEG-BDB). Four derivatives with various oligo-Arg lengths were prepared, and the effect of oligo-Arg length on the gene delivery efficacy was investigated in HeLa cells. We demonstrate that the arginine 10-mer exhibits the highest transfection efficiency in HeLa cells among our series of compounds.

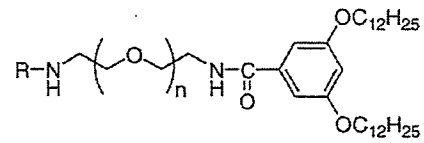

1 R = H
2 R = Fmoc-Arg(Pmc)
3 R = Arg(Pmc)
4 R = Fmoc-[Arg(Pmc)]$_2$
5 R = [Arg(Pmc)]$_2$
6 R = Fmoc-[Arg(Pmc)]$_3$
7 R = [Arg(Pmc)]$_3$
8 R = Fmoc-[Arg(Pmc)]$_4$
9 R = Arg_4 (Arg4-PEG-BDB)
10 R = Fmoc-[Arg(Pbf)]$_6$
11 R = Arg_6 (Arg6-PEG-BDB)
12 R = Fmoc-[Arg(Pbf)]$_6$[Arg(Pmc)]$_2$
13 R = Arg_8 (Arg8-PEG-BDB)
14 R = [Arg(Pmc)]$_4$
15 R = Fmoc-[Arg(Pbf)]$_6$[Arg(Pmc)]$_4$
16 R = Arg_{10} (Arg10-PEG-BDB)

Fig. 1. Chemical structures of ArgN-PEG-BDBs and their synthetic intermediates.

2. Materials and methods

2.1. Materials

All amino acid derivatives and coupling reagents were obtained from Kokusan chemical Co., LTD (Tokyo, Japan). PEG 2000 was obtained from Kanto Kagaku Co., Ltd (Tokyo, Japan), and converted into its diamino derivative using a reported procedure (Slama and Rando, 1980). 9-fluorenylmethyloxycarbonyl-[Arg(2,2,4,6,7-pentamethyldihydrobenzofuran-5-sulfonyl)]$_6$-OH (Fmoc-[Arg(Pbf)]$_6$-OH) was purchased from Peptide Institute, Inc (Osaka, Japan). The Pica gene luciferase assay kit was purchased from Toyo Ink (Tokyo, Japan). Bicinchonic acid (BCA) protein assay reagent and EZ-Label Fluorescein Protein Labeling Kit were obtained from Pierce (Rockford, IL, USA). Lipofectamine^{TM} 2000, fluorescein isothiocyanate (FITC)-transferrin and Dulbecco's modified Eagle's medium (DMEM) were purchased from Invitrogen Corp. (Carlsbad, CA, USA). FITC-Tat was purchased from AnaSpec, Inc. (San Jose, CA, USA). All other chemicals used were of reagent grade. Fetal bovine serum (FBS) was purchased from Life Technologies (Grand Island, NY, USA). In the following section, the number of moles of PEG in compounds is calculated by taking the molecular weight of the PEG fragment as 2000.

2.2. Synthesis of oligo-Arg-PEG-BDBs

3,5-Bis(dodecyloxy)benzoic acid (Balagurusamy et al., 1997) (1 g) and benzotriazol-1-yl-oxy-tris-pyrrolidino-phosphonium hexafluorophosphate (PyBOP) (0.38 g) were dissolved in *N,N*-dimethylformamide (DMF) (30 mL), and the solution was stirred at room temperature for 1 h. Diamino poly(ethylene glycol) 2000 (5 g) was added to the solution, and the reaction was carried out overnight. The resulting mixture was poured into water, and extracted with $CHCl_3$. The organic layer was washed with water, dried over $MgSO_4$, and filtered, and the organic solvent was evaporated under reduced pressure. The residue was purified by silica gel column chromatography to give **1** (Fig. 1). Fmoc-Arg(2,2,5,7,8-pentamethylchroman-6-sulfonyl (Pmc))-OH (1.07 g) and PyBOP (0.84 g) were dissolved in DMF (20 mL), and the solution was stirred at room temperature for 1 h. **1** (2 g) was added to the solution, and the reaction was carried out overnight. The resulting mixture was poured into water, and extracted with $CHCl_3$. The organic layer was washed with water, dried over $MgSO_4$, filtered, and the organic solvent was evaporated under reduced pressure. The residue was purified by Sephadex LH-20 to give **2**. To a solution of **2** (2.45 g) in CH_2Cl_2, piperidine was added, and the solution was stirred at room temperature for 30 min. The resulting mixture was directly purified using Sephadex LH-20 to give **3**. Similarly, **4**, **5**, **6**, **7** and **8** were synthesized step by step. A solution of **8** (0.2 g) in trifluoroacetic acid (TFA)/water (9/1, 2 mL) was stirred at room temperature for 3 h, and concentrated in vacuo. The residue was dissolved in CH_2Cl_2. Piperidine was added to the solution, and the reaction carried out at room temperature for 30 min. The resulting mixture was directly purified by silica gel column chromatography to give Arg4-PEG-BDB (**9**). MALDI-TOF MS (α-CHCA) 3096.13, 3140.03, 3184.71 ($[M+H]^+$). Similar to the synthesis of **2** and **8**, **10** and Arg6-PEG-BDB (**11**), respectively, were synthesized from Fmoc-[Arg(Pbf)]$_6$-OH and **1**. MALDI-TOF MS (α-CHCA) 3584.62, 3628.17, 3672.29 ($[M+H]^+$). Similar to the synthesis of **2** and **8**, **12** and Arg8-PEG-BDB (**13**), respectively, were synthesized from Fmoc-[Arg(Pbf)]$_6$-OH and **5**. MALDI-TOF MS (α-CHCA) 3670.02, 3714.17, 3757.87 ($[M+H]^+$). Similar to the deprotection of the Fmoc group of **2** and **8** gave **14**. Similar to the synthesis of **2** and **8**, **15** and Arg10-PEG-BDB (**16**), respectively, were synthesized from Fmoc-[Arg(Pbf)]$_6$-OH and **14**. MALDI-TOF MS (α-CHCA) 4123.36, 4166.18, 4209.92 ($[M+H]^+$).

2.3. Plasmid DNA and FITC-labeled oligodeoxynucleotide

The plasmid DNA (about 6740 bp) encoding the luciferase gene under the control of the CMV promoter (pCMV-luc) was supplied by Dr. Tanaka of the Mt. Sinai School of Medicine (NY, USA). The plasmid pEGFP-C1 encoding the green fluorescent protein (GFP) under the CMV promoter was purchased from Clontech (Palo Alto, CA, USA). Protein-free preparations of pCMV-luc and pEGFP-C1 were purified following alkaline lysis using maxiprep columns (Qiagen, Hilden, Germany). The

FITC-labeled 20-mer randomized oligodeoxynucleotide (FITC-labeled ODN) was synthesized with a phosphodiester backbone (Sigma Genosys Japan, Hokkaido, Japan).

2.4. Preparation of FITC-labeled Arg10-PEG-BDB

FITC-labeled Arg10-PEG-BDB was prepared by applying an EZ-Label Fluorescein Protein Labeling Kit to Arg10-PEG-BDB.

2.5. Cell culture

Human cervical carcinoma cells (HeLa) were kindly provided by Toyobo Co., Ltd. (Osaka, Japan). HeLa cells were grown in DMEM supplemented with 10% FBS at 37 °C in a humidified 5% CO_2 atmosphere.

2.6. Gene transfection

An aqueous solution of plasmid DNA (pCMV-luc or pEGFP-C1) or FITC-labeled ODN was added to the oligo-Arg-PEG-BDB aqueous solution with gentle shaking to form oligo-Arg-PEG-BDB/DNA complexes. Each complex was left at room temperature for 10–15 min. HeLa cell cultures were prepared by plating cells in a 35-mm culture dish 24 h prior to each experiment. The cells were washed 3 times with 1 mL of serum-free DMEM. For transfection, each oligo-Arg-PEG-BDB/DNA complex (2 μg of plasmid DNA and 100 μg of oligo-Arg-PEG-BDB per well were fixed with a charge ratio (+/−) of oligo-Arg to plasmid DNA of 4.25–5.5 (Arg4-PEG-BDB-Arg10-PEG-BDB)) was diluted with serum-free DMEM to 1 mL, then gently applied to the cells. Two sets of conditions were employed: (a) after incubation for 3 h at 37 °C in serum-free DMEM, DMEM (1 mL) containing 10% FBS was added, and the cells were further incubated for 21 h, (b) incubation for 24 h at 37 °C in DMEM (2 mL) containing 10% FBS. For transfection with Lipofectamine™ 2000, 5 μL of Lipofectamine™ 2000 was used for 2 μg of the plasmid DNA to form a DNA complex in Opti-MEM according to the manufacturer's protocol. The incubation conditions were the same as stated above. The measurement of gene transfer efficiency was performed in triplicate.

2.7. Inhibition of endocytosis

Arg10-PEG-BDB (100 μg) containing 20% FITC-labeled Arg10-PEG-BDB or its complex with plasmid DNA (2 μg), FITC-transferrin and FITC-Tat were diluted with DMEM containing 10% FBS to 1 mL and then incubated with cells for 3 h at either 4 °C or 37 °C.

2.8. Luciferase assay

Luciferase expression was measured according to the instructions accompanying the luciferase assay system. Incubation was terminated by washing the plates three times with cold phosphate buffered saline (pH 7.4) (PBS). Cell lysis solution (Pica gene) was added to the cell monolayers and subjected to freezing at −80 °C and thawing at 37 °C, followed by centrifugation at 15,000 rpm for 5 s. The supernatants were frozen and stored at −80 °C until the assays. Aliquots of 20 μL of the supernatants were mixed with 100 μL of luciferase assay system (Pica gene) and counts per second (cps) were measured with a chemoluminometer (Wallac ARVO SX 1420 multilabel counter, Perkin-Elmer Life Science, Japan, Co. Ltd., Kanagawa, Japan). The protein concentration of the supernatants was determined with BCA reagent using bovine serum albumin as a standard and cps/μg protein was calculated.

2.9. Flow cytometry

At the end of the incubation, the dishes were washed two times with 1 mL of PBS, and the cells were detached with 0.05% trypsin and EDTA solution. The cells were centrifuged at 1500×*g*, and the supernatant was discarded. The cells were resuspended with PBS containing 0.1% BSA and 1 mM EDTA, and directly introduced to a FACSCalibur flow cytometer (Becton Dickinson, San Jose, CA, USA) equipped with a 488 nm argon ion laser. Data for 10,000 fluorescent events were obtained by recording forward scatter (FSC) and side scatter (SSC) with green (530/30 nm) fluorescence.

2.10. Confocal microscopy

GFP expression in HeLa cells was observed after the gene transfection with incubation for 3 h at 37 °C in serum-free DMEM. DMEM (1 mL) containing 10% FBS was added as described above. After the medium was removed, the cells were washed with PBS and fixed with 10% formaldehyde PBS at room temperature for 20 min, and washed three times with PBS. Then, the cells were coated with Aqua Poly/Mount (Poly science, Warrington, PA, USA) to prevent fading and covered with coverslips. The fixed cells were observed with a Radiance 2100 confocal laser scanning microscope (BioRad, CA, USA). GFP was imaged using the 488-nm excitation beam of an argon laser, and fluorescence emission was observed with a filter HQ515/30. The contrast level and brightness of the images were adjusted.

2.11. Particle size determination

The oligo-Arg-PEG-BDB/DNA complex and Lipofectamine™ 2000/DNA complex were formed as described in Gene Transfection. Particle size was measured by the dynamic light-scattering method (ELS-800, Otsuka Electronics Co. Ltd, Osaka, Japan) at 25 °C after diluting the Arg-PEG-BDB/DNA complex, the Lipofectamine™ 2000/DNA complex, Lipofectamine™ 2000 and Arg10-PEG-BDB to an appropriate volume with Milli-Q water.

2.12. Cytotoxicity

HeLa cells were seeded at a density of 1×10^4 cells per well in 96-well plates and maintained for 24 h before transfection in DMEM supplemented with 10% FBS. The cells were washed

with serum-free DMEM. The culture medium was replaced with serum-free DMEM (50 μL) including various concentrations of Arg10-PEG-BDB ranging from 2.5 to 1000 μM, or the DNA complex as described in Section 2.6. After incubation for 3 h at 37 °C with serum-free DMEM (50 μL), DMEM (50 μL) containing 10% FBS was added. The cells were further incubated for 21 h. The number of surviving cells was determined by a WST-8 assay (Dojindo Laboratories, Kumamoto, Japan). Cell viability was expressed as the ratio of the A_{450} of cells treated with the DNA complex to that of the control samples.

2.13. Data analysis

Significant differences in the mean values were evaluated by student's unpaired *t*-test. A *p*-value of less than 0.05 was considered significant.

3. Results

3.1. Luciferase expression of Arg-PEG-BDB/DNA complexes

We prepared four oligo-Arg-linked lipids of various lengths, Arg4-PEG-BDB, Arg6-PEG-BDB, Arg8-PEG-BDB and Arg10-PEG-BDB (Fig. 1). We evaluated the transfection efficiency of oligo-Arg-PEG-BDB by assaying luciferase activity. HeLa cells were transfected with oligo-Arg-PEG-BDB complexed with pCMV-luc. Transfection was conducted for 3 h in the absence or presence of serum, and the cells were cultured for another 21 h in the presence of serum. According to the result of a preliminary experiment, the oligo-Arg-PEG-BDB concentration appeared to be an important factor in obtaining a high transfection efficiency. All oligo-Arg-PEG-BDB derivatives exhibited luciferase activity at 40 μg/mL with a charge ratio of cation to plasmid of 2.2–1.7 (Arg4-PEG-BDB-Arg10-PEG-BDB). As the concentration of oligo-Arg-PEG-BDB increased, the level of luciferase activity also increased. However, it was observed that Arg8-PEG-BDB became cytotoxic at 200 μg/mL in the gene transfection. Therefore, the concentration of oligo-Arg-PEG-BDB should be restricted. A concentration of 100 μg/mL, corresponding to 32, 29, 27 and 25 μM for Arg4-PEG-BDB, Arg6-PEG-BDB, Arg8-PEG-BDB and Arg10-PEG-BDB, respectively, was used in the subsequent experiments.

Fig. 2(A) and (B) demonstrates that the longer oligo-Arg showed stronger luciferase activity irrespective of the serum in the medium. Arg10-PEG-BDB showed the highest level of activity among the oligo-Arg-PEG-BDB derivatives, with about 40-fold, 11-fold and 4-fold higher transfection efficiencies than Arg4-PEG-BDB, Arg6-PEG-BDB and Arg8-PEG-BDB, respectively, on 3 h-incubation in serum-free medium (Fig. 2(A)). Arg10-PEG-BDB showed about 1/5 the transfection efficiency of Lipofectamine™ 2000, a commercial gene transfection reagent, even in a serum-containing medium (Fig. 2(B)). Serum tended to decrease the gene transfection efficiency of oligo-Arg-PEG-BDB, an exception being Arg10-PEG-BDB.

3.2. Cellular uptake of Arg-PEG-BDB/DNA complexes

To confirm the ability of oligo-Arg-PEG-BDB to carry genes into cells, we prepared ODN labeled with FITC and assayed the cell internalization of the Arg8-PEG-BDB, Arg10-PEG-BDB/ODN or Lipofectamine™ 2000 complex by flow cytometry (Fig. 3). Cells were exposed for 3 h to the FITC-labeled ODN complex in the absence (Fig. 3(A)) or presence of serum (Fig. 3(B)), cultured for another 21 h in the presence of serum, and then trypsinized. A flow cytometric analysis demonstrated that cell internalization occurred in each case and in the absence of serum, Lipofectamine™ 2000 showed the strongest labeling

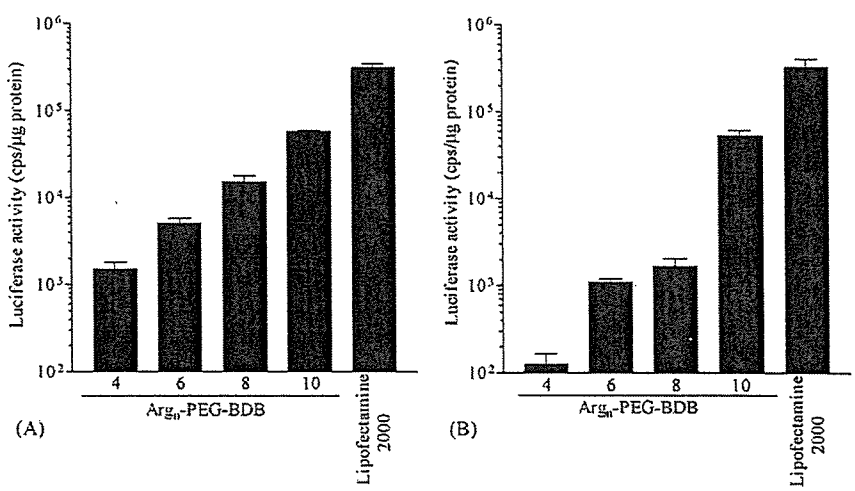

Fig. 2. In vitro luciferase activity after transfection of HeLa cells using oligo-Arg-PEG-BDB/DNA complexes. The complexes were prepared by mixing 2 μg of pCMV-luc with 100 μg of oligo-Arg-PEG-BDB or Lipofectamine™ 2000 (5 μL). The charge ratio of cation to plasmid was 4.25–5.5 (Arg4-PEG-BDB-Arg10-PEG-BDB). (A) After incubation for 3 h at 37 °C in serum-free DMEM, DMEM (1 mL) containing 10% FBS was added, and the cells were further incubated for 21 h. (B) Cells were incubated for 24 h at 37 °C in DMEM (2 mL) containing 10% FBS. Each bar represents the mean ± S.D. of three experiments.

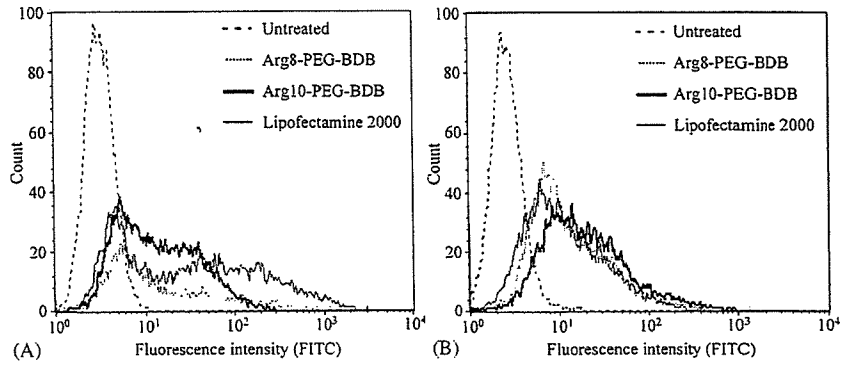

Fig. 3. Cellular uptake of the DNA complexes of Arg8-PEG-BDB and Arg10-PEG-BDB. Arg8-PEG-BDB, Arg10-PEG-BDB (100 μg) or Lipofectamine™ 2000 was mixed with 2 μg of FITC-labeled ODN. (A) The cells were incubated for 3 h in serum-free DMEM and incubated another 21 h in DMEM containing 10% FBS. (B) The cells were incubated for 24 h in DMEM (2 mL) containing 10% FBS and treated with trypsin before FACS analysis. Rough dotted line, untreated; Subtle dotted line, Arg8-PEG-BDB; Bold line, Arg10-PEG-BDB; Plain line, Lipofectamine™ 2000.

intensity among vectors. However, in the presence of serum, the intensity of the signal was greater in the cells transfected with Arg10-PEG-BDB than those with Lipofectamine™ 2000 and Arg8-PEG-BDB, indicating that Arg10-PEG-BDB could carry more DNA into the cells than Lipofectamine™ 2000 and Arg8-PEG-BDB. It suggests that the uptake efficiency of Arg10-PEG-BDB was not susceptible to the serum. These results suggest that the optimal number of oligo-Arg was 10 among the tested. Therefore, Arg10-PEG-BDB was used in subsequent experiments.

3.3. GFP gene transfection

To examine the distribution of transfection in cells, we observed the transfection efficiency of Arg10-PEG-BDB with the plasmid pEGFP-C1 using confocal microscopy. Cells were exposed for 3 h to the Arg10-PEG-BDB or Lipofectamine™ 2000/DNA complex in the absence of serum, and then cultured for another 21 h in the presence of serum. Next, the cells were fixed with 10% paraformaldehyde and visualized by confocal microscopy (Fig. 4). A slightly lower level of GFP protein was observed in the cells treated with Arg10-PEG-BDB than with Lipofectamine™ 2000, corresponding to the results of luciferase expression (Fig. 2). Similar results were obtained in a flow cytometric study for Arg10-PEG-BDB and Lipofectamine™ 2000 in serum-free incubation (Fig. 3(A)).

3.4. Effect of low temperature on the uptake

To confirm the internalization mechanism of our CPP, we prepared FITC-labeled Arg10-PEG-BDB and examined the effect of temperature on the cellular uptake of complexes. In order to avoid changes in the cell internalization character, we only incorporated FITC-labeled Arg10-PEG-BDB (20%). The endocytosis marker transferrin (Tf) and another CPP of Tat were used as control. The cells were exposed to FITC-labeled Arg10-PEG-BDB or its DNA complex, FITC-transferrin and FITC-Tat for 3 h at either 4 °C or 37 °C in the presence of serum. Then, the cells were trypsinized and analyzed by flow cytometry (Fig. 5). FITC-labeled Arg10-PEG-BDB and its DNA complex showed about an 86% lower internalization efficiency at 4 °C than at 37 °C. No significant difference in the mean fluorescence was observed between the DNA complex and FITC-labeled Arg10-PEG-BDB alone at 4 and 37 °C (Fig. 5(C)). This finding suggests that the internalization by our oligo-Arg-PEG-BDB and its DNA complexes was considerably inhibited at low temperature.

3.5. Particle size

Particle sizes of Arg10-PEG-BDB, Lipofectamine™ 2000, Arg10-PEG-BDB/DNA and Lipofectamine™ 2000/DNA were estimated using dynamic light scattering in Milli-Q water 15–60 min after the complex had formed. Particles of

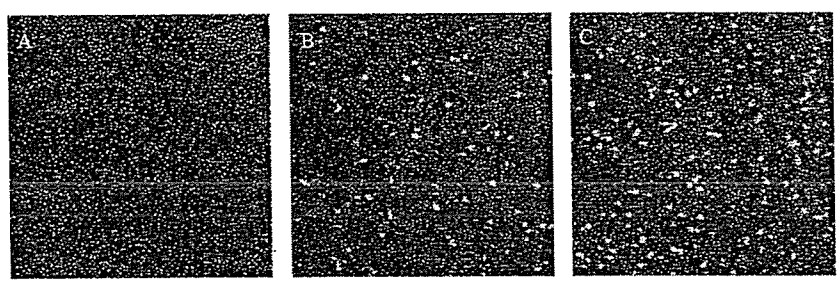

Fig. 4. Analysis of GFP expression by confocal microscopy. The DNA complexes were prepared by mixing 2 μg of pEGFP with Arg10-PEG-BDB (100 μg) or Lipofectamine™ 2000 (5 μL). The cells were incubated for 3 h in serum-free DMEM and incubated another 21 h in DMEM (1 mL) containing 10% FBS before confocal microscopy. Panel A, untreated; panel B, Arg10-PEG-BDB; panel C, Lipofectamine™ 2000. All views were recorded with the same camera acquisition parameters.

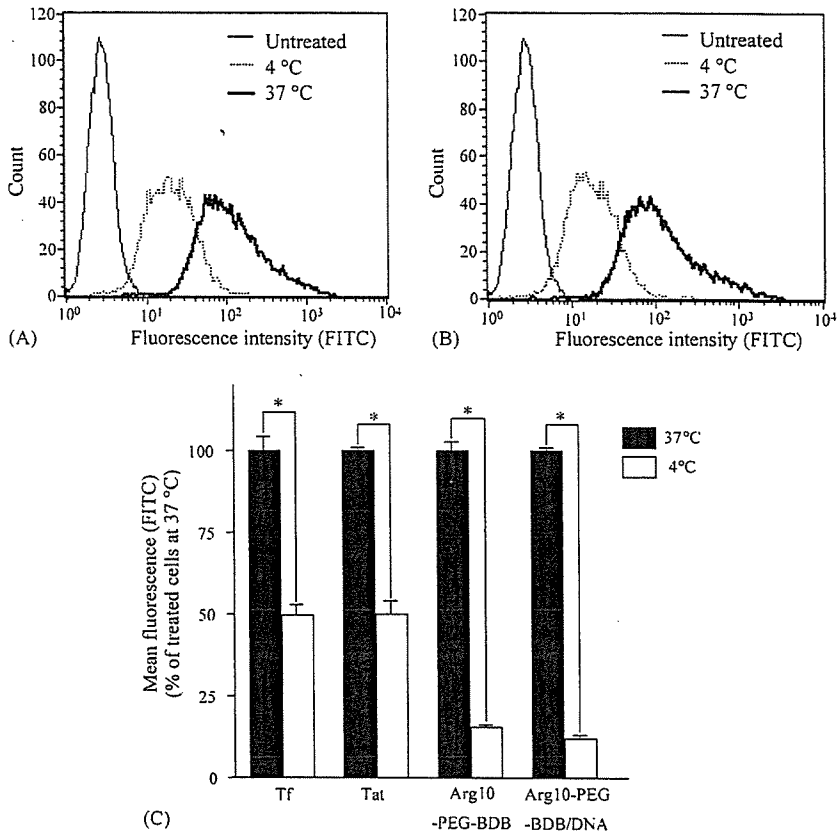

Fig. 5. Effect of temperature on the cellular uptake of FITC-labeled Arg10-PEG-BDB and its DNA complexes. (A) Arg10-PEG-BDB containing 20% FITC-labeled Arg-PEG-BDB. (B) The complex of plasmid DNA with FITC-labeled Arg10-PEG-BDB. Arg10-PEG-BDB was labeled with fluorescein isothiocyanate at the N-terminal of oligo-Arg as described under experimental procedures. The DNA complexes were prepared by mixing 2 μg of plasmid DNA with FITC-labeled Arg10-PEG-BDB (100 μg). The cells were incubated for 3 h at 4 or 37 °C in DMEM (1 mL) containing 10% FBS, and treated with trypsin before flow cytometry. (C) The mean fluorescence intensity of FITC-labeled Arg10-PEG-BDB, its DNA complexes, FITC-transferrin (Tf) (25 μg/mL) and FITC-Tat (Tat) (10 μM) compared with treated cells at 37 and 4 °C. Closed bar, 37 °C; Open bar, 4 °C. Each bar represents the mean ± S.D. of three experiments. $p < 0.05$ are marked by asterisk.

Arg10-PEG-BDB and the Arg10-PEG-BDB/DNA complex were about 300 and 1000 nm, respectively, suggesting that Arg10-PEG-BDB formed micelles. Those of Lipofectamine™ 2000 and the Lipofectamine™ 2000/DNA complex were about 400 nm and about 800 nm, respectively.

3.6. Cytotoxicity

The cytotoxicity of the vectors was assessed by the WST-8 assay using cells incubated with Arg10-PEG-BDB in serum-free medium for 3 h and in a serum-containing medium for another 21 h. The IC_{50} value was about 550 μM for Arg10-PEG-BDB (data not shown). The cytotoxicity of the Arg10-PEG-BDB/DNA complex was almost equal to that of the Lipofectamine™ 2000/DNA complex in both sets of conditions (Fig. 6).

4. Discussion

A peptide consisting of oligo-Arg has been shown to be translocated through cell membranes as efficiently as other CPPs (Mitchell et al., 2000; Wender et al., 2000; Futaki et al., 2001a). In these cases, the oligo-Arg length and the hydrophobic moiety of oligo-Arg conjugates were important factors for the uptake and transfection in cells (Futaki et al., 2001b). The aims of this study were to design and synthesize novel oligo-Arg-linked PEG-lipids, and determine the optimal length of oligo-Arg for transfection efficiency and to develop an effective gene delivery vector.

We prepared oligo-Arg-modified lipids with a PEG linker. The transfection experiment using pCMV-luc showed the ability of oligo-Arg-PEG-BDB to carry genes into cells. The transfection efficiency of the longer oligo-Arg was higher. The transfection efficiency in the absence of serum increased about four times as two arginine residues were added. The highest level of luciferase activity in cells was observed in Arg10-PEG-BDB irrespective of serum, suggesting that the optimal number of arginine residues for transfection was 10.

A limitation of the transfection assay with pCMV-luc is that it does not provide any information on the percentage of cells transfected. Therefore, we used pEGFP-C1 as another plasmid DNA. Arg10-PEG-BDB showed a similar efficiency in gene transfer to pCMV-luc, and a slightly lower fluorescence to Lipofectamine™ 2000, on confocal microscopy and flow cytometry in serum-free medium. The transfection assay with pEGFP-C1 and Arg10-PEG-BDB provided evidence that the

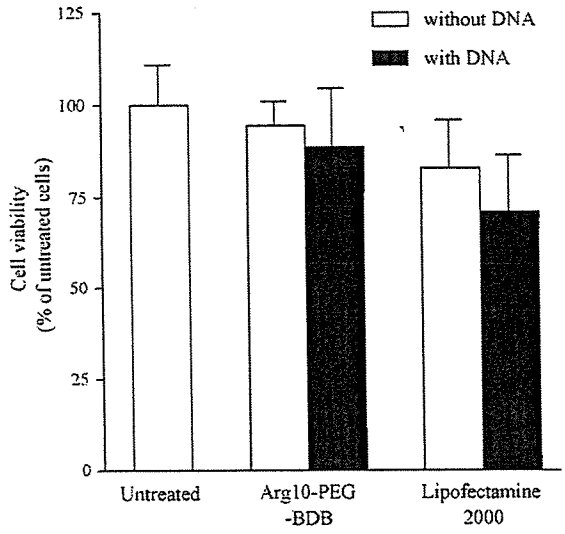

Fig. 6. Cytotoxicity of Arg10-PEG-BDB and Lipofectamine™ 2000 complexed with the plasmid DNA. The cytotoxicity on transfection was evaluated using the WST-8 assay. HeLa cells were seeded at a density of 1×10^4 cells per well in 96-well plates and maintained for 24 h before the gene transfection in DMEM containing 10% FBS. The culture medium was replaced with serum-free DMEM (50 μL) containing DNA (2 μg) complexed with Arg10-PEG-BDB (100 μg) or with Lipofectamine™ 2000 (5 μL). After incubation for 3 h at 37 °C in DMEM without FBS, DMEM (50 μL) containing 10% FBS was added. The cells were further incubated for another 21 h. Open bars, cell viability in the absence of plasmid DNA; Closed bars, cell viability in the presence of plasmid DNA. Each bar represents the mean ± S.D. of three experiments.

observed transfection efficiency resulted from low overall levels of gene insertion in many cells, not from a low overall percentage of cells transfected with a few cells receiving large numbers of the reporter gene.

We also showed that both Arg8-PEG-BDB and Arg10-PEG-BDB were able to carry plasmid DNA inside the cells by flow cytometry. To removing the surface bound Arg-PEG-BDB/DNA complexes, we washed the cells with PBS and treated them with trypsin (Richard et al., 2003). In the presence of serum, Arg10-PEG-BDB was able to deliver more DNA into the cells than Lipofectamine™ 2000 and Arg8-PEG-BDB, but this finding did not reflect in transfection efficiency. It was suggested that the process of cellular uptake and/or transfection might be different between Arg10-PEG-BDB and Lipofectamine™ 2000. No severe cytotoxicity was observed during 24 h incubation at 25 μM (100 μg/mL) of Arg10-PEG-BDB (Fig. 6). Notably, even in the presence of serum, the Arg10-PEG-BDB/DNA complex achieved appreciable cellular association to attain a high level of gene expression.

Mitchell et al. reported that 15 arginine residues were internalized significantly more effectively than 20 arginine residues (Mitchell et al., 2000). Wender et al. reported that nine arginine residues, the maximum number used in their experiment, were superior to shorter oligomers in terms of cellular uptake as determined by flow cytometry (Wender et al., 2000). They also demonstrated that the presence of at least six arginine residues is important for cellular uptake (Wender et al., 2000). Using oligomers composed of 4–16 arginine residues, Futaki et al. demonstrated that there was an optimal number of arginine residues (Arg8) for cellular internalization by microscopic observation (Futaki et al., 2001a). They also reported that stearylation of Arg8 at the N-terminal (stearyl-Arg8) improved the transfection efficiency compared with Arg8 alone, giving the highest transfection efficiency from stearyl-Arg4 to stearyl-Arg16 at a charge ratio of cation to DNA of 2:1 (Futaki et al., 2001b). In our case, Arg10-PEG-BDB showed a higher transfection efficiency and cellular uptake than Arg8-PEG-BDB.

Therefore, effect of the length of oligo-Arg on transfection efficiency has to be taken into consideration. In transfection experiments with the oligo-Arg-PEG-BDB/DNA complex, the arginine residues may be partly used for translocation through the plasma membrane and partly for the formation of complex with plasmid DNA. The longer oligo-Arg would be needed for the intracellular delivery of oligo-Arg-PEG-BDB/DNA than the uptake of oligo-Arg-PEG-BDB alone. In this respect, oligo-Arg-PEG-BDB with more than ten arginine residues would be more effective for transfection if no cytotoxicity is observed. Cytotoxicity may be influenced by incubation with or without serum and/or cell type. The cellular uptake and transfection efficiency of oligo-Arg-PEG-BDB/DNA complexes were proportional to the chain length of oligo-Arg. This finding suggests that the limiting factor of gene transfection was the uptake of complex to the plasma membrane, and not the release of DNA from the endosome compartment to the cell cytoplasm or the penetration of DNA into the nucleus.

It is interesting that two quite different designs of oligo-Arg-lipids, Arg10-PEG-BDB (25 μM) (Fig. 2) and stearyl-Arg8 (30 μM) (Futaki et al., 2001b), showed comparable transfection efficiencies to Lipofectamine™ 2000. The presence of a PEG linker and the lipid structure does not seem to affect the length of oligo-Arg suitable for the transfection and uptake. The transfection efficiency is likely to be influenced more by the length of oligo-Arg than by overall structural features such as the anchor lipids, linker groups, and direction of oligo-Arg relative to the lipid portion, etc.

The cellular translocation by CPP was initially proposed to be an energy-independent process. Most papers report no difference in uptake between 37 and 4 °C (Vives et al., 1997; Futaki et al., 2001a). However, more recent papers suggest that the majority of the translocation occurs via an energy-dependent pathway and that the translocation of CPP is reduced by endocytosis inhibitors (Fischer et al., 2002; Vives, 2003; Drin et al., 2003). To investigate the internalization mechanism of our system, we constructed FITC-labeled Arg10-PEG-BDB and its DNA complex, and examined the temperature-dependence of their internalization using flow cytometry. Therefore, the internalization mechanism of our system may have less of a contribution from energy-independent processes. FITC-labeled Arg10-PEG-BDB alone showed a similar internalization efficiency to the FITC-labeled Arg10-PEG-BDB/DNA complex at 37 °C for 3 h, suggesting that Arg10-PEG-BDB and Arg10-PEG-BDB/DNA follow a similar pathway. These findings conflict with the report that the quantitative uptake of free CPP or CPP coupled to cargo can differ (Fischer et al., 2004), but corresponds to the report that the cellular entry of both stearyl-Arg8 and the stearyl-Arg8/DNA

complex occurs mainly through endocytosis (Khalil et al., 2004).

Given the particle size of Arg10-PEG-BDB, aggregates such as micelles would be formed since PEG-lipid conjugates were reported to form micelles (Lukyanov et al., 2002). One explanation for the transfection efficiency of Arg10-PEG-BDB could be that Arg10-PEG-BDB aggregates and behaves similarly to polycationic micelles (Itaka et al., 2003).

5. Conclusions

In summary, we synthesized oligo-Arg containing lipids with a PEG spacer as novel gene vectors, and found that their transfection efficiency increased as the number of arginine residues increased. Among them, Arg10-PEG-BDB showed the highest transfection efficiency in HeLa cells. Arg10-PEG-BDB and its DNA complex may be internalized via energy-dependent processes.

Acknowledgements

This project was supported in part by a grant from the Promotion and Mutual Aid Corporation for Private Schools of Japan and by a Grant-in-Aid for Scientific Research from the Ministry of Education, Culture, Sports, Science, and Technology of Japan.

References

Balagurusamy, V.S.K., Ungar, G., Percec, V., Johansson, G., 1997. Rational design of the first spherical supramolecular dendrimers self-organized in a novel thermotropic cubic liquid-crystalline phase and the determination of their shape by X-ray analysis. J. Am. Chem. Soc. 119, 1539–1555.

Brown, M.D., Schatzlein, A., Brownlie, A., Jack, V., Wang, W., Tetley, L., Gray, A.I., Uchegbu, I.F., 2000. Preliminary characterization of novel amino acid based polymeric vesicles as gene and drug delivery agents. Bioconjug. Chem. 11, 880–891.

Cotten, M., Langle-Rouault, F., Kirlappos, H., Wagner, E., Mechtler, K., Zenke, M., Beug, H., Birnstiel, M.L., 1990. Transferrin–polycation-mediated introduction of DNA into human leukemic cells: stimulation by agents that affect the survival of transfected DNA or modulate transferrin receptor levels. Proc. Natl. Acad. Sci. U.S.A. 87, 4033–4037.

Derossi, D., Joliot, A.H., Chassaing, G., Prochiantz, A., 1994. The third helix of the antennapedia homeodomain translocates through biological membranes. J. Biol. Chem. 269, 10444–10450.

Drin, G., Cottin, S., Blanc, E., Rees, A.R., Temsamani, J., 2003. Studies on the internalization mechanism of cationic cell-penetrating peptides. J. Biol. Chem. 278, 31192–31201.

Felgner, P.L., Gadek, T.R., Holm, M., Roman, R., Chan, H.W., Wenz, M., Northrop, J.P., Ringold, G.M., Danielsen, M., 1987. Lipofection: a highly efficient, lipid-mediated DNA-transfection procedure. Proc. Natl. Acad. Sci. U.S.A. 84, 7413–7417.

Fischer, R., Waizenegger, T., Kohler, K., Brock, R., 2002. A quantitative validation of fluorophore-labelled cell-permeable peptide conjugates: fluorophore and cargo dependence of import. Biochim. Biophys. Acta 1564, 365–374.

Fischer, R., Kohler, K., Fotin-Mleczek, M., Brock, R., 2004. A stepwise dissection of the intracellular fate of cationic cell-penetrating peptides. J. Biol. Chem. 279, 12625–12635.

Futaki, S., Suzuki, T., Ohashi, W., Yagami, T., Tanaka, S., Ueda, K., Sugiura, Y., 2001a. Arginine-rich peptides. An abundant source of membrane-permeable peptides having potential as carriers for intracellular protein delivery. J. Biol. Chem. 276, 5836–5840.

Futaki, S., Ohashi, W., Suzuki, T., Niwa, M., Tanaka, S., Ueda, K., Harashima, H., Sugiura, Y., 2001b. Stearylated arginine-rich peptides: a new class of transfection systems. Bioconjug. Chem. 12, 1005–1011.

Itaka, K., Yamauchi, K., Harada, A., Nakamura, K., Kawaguchi, H., Kataoka, K., 2003. Polyion complex micelles from plasmid DNA and poly(ethylene glycol)-poly(L-lysine) block copolymer as serum-tolerable polyplex system: physicochemical properties of micelles relevant to gene transfection efficiency. Biomaterials 24, 4495–4506.

Khalil, I.A., Futaki, S., Niwa, M., Baba, Y., Kaji, N., Kamiya, H., Harashima, H., 2004. Mechanism of improved gene transfer by the N-terminal stearylation of octaarginine: enhanced cellular association by hydrophobic core formation. Gene Ther. 11, 636–644.

Kircheis, R., Schuller, S., Brunner, S., Ogris, M., Heider, K.H., Zauner, W., Wagner, E., 1999. Polycation-based DNA complexes for tumor-targeted gene delivery in vivo. J. Gene Med. 1, 111–120.

Lewin, M., Carlesso, N., Tung, C.H., Tang, X.W., Cory, D., Scadden, D.T., Weissleder, R., 2000. Tat peptide-derivatized magnetic nanoparticles allow in vivo tracking and recovery of progenitor cells. Nat. Biotechnol. 18, 410–414.

Lukyanov, A.N., Gao, Z., Mazzola, L., Torchilin, V.P., 2002. Polyethylene glycol-diacyllipid micelles demonstrate increased acculumation in subcutaneous tumors in mice. Pharm. Res. 19, 1424–1429.

Mitchell, D.J., Kim, D.T., Steinman, L., Fathman, C.G., Rothbard, J.B., 2000. Polyarginine enters cells more efficiently than other polycationic homopolymers. J. Pept. Res. 56, 318–325.

Morris, M.C., Depollier, J., Mery, J., Heitz, F., Divita, G., 2001. A peptide carrier for the delivery of biologically active proteins into mammalian cells. Nat. Biotechnol. 19, 1173–1176.

Oehlke, J., Scheller, A., Wiesner, B., Krause, E., Beyermann, M., Klauschenz, E., Melzig, M., Bienert, M., 1998. Cellular uptake of an alpha-helical amphipathic model peptide with the potential to deliver polar compounds into the cell interior non-endocytically. Biochim. Biophys. Acta 1414, 127–139.

Pooga, M., Hallbrink, M., Zorko, M., Langel, U., 1998. Cell penetration by transportan. FASEB J. 12, 67–77.

Richard, J.P., Melikov, K., Vives, E., Ramos, C., Verbeure, B., Gait, M.J., Chernomordik, L.V., Lebleu, B., 2003. Cell-penetrating peptides. A reevaluation of the mechanism of cellular uptake. J. Biol. Chem. 278, 585–590.

Schwarze, S.R., Ho, A., Vocero-Akbani, A., Dowdy, S.F., 1999. In vivo protein transduction: delivery of a biologically active protein into the mouse. Science 285, 1569–1572.

Slama, J.S., Rando, R.R., 1980. Lectin-mediated aggregation of liposomes containing glycolipids with variable hydrophilic spacer arms. Biochemistry 19, 4595–4600.

Song, Y.K., Liu, F., Liu, D., 1998. Enhanced gene expression in mouse lung by prolonging the retention time of intravenously injected plasmid DNA. Gene Ther. 5, 1531–1537.

Torchilin, V.P., Rammohan, R., Weissig, V., Levchenko, T.S., 2001. TAT peptide on the surface of liposomes affords their efficient intracellular delivery even at low temperature and in the presence of metabolic inhibitors. Proc. Natl. Acad. Sci. U.S.A. 98, 8786–8791.

Vives, E., 2003. Cellular uptake of the Tat peptide: an endocytosis mechanism following ionic interactions. J. Mol. Recognit. 16, 265–271.

Vives, E., Brodin, P., Lebleu, B., 1997. A truncated HIV-1 Tat protein basic domain rapidly translocates through the plasma membrane and accumulates in the cell nucleus. J. Biol. Chem. 272, 16010–16017.

Wender, P.A., Mitchell, D.J., Pattabiraman, K., Pelkey, E.T., Steinman, L., Rothbard, J.B., 2000. The design, synthesis, and evaluation of molecules that enable or enhance cellular uptake: peptoid molecular transporters. Proc. Natl. Acad. Sci. U.S.A. 97, 13003–13008.

Available online at www.sciencedirect.com
SCIENCE DIRECT
Journal of Controlled Release 113 (2006) 146–154
journal of controlled release
www.elsevier.com/locate/jconrel

Novel ultra-deformable vesicles entrapped with bleomycin and enhanced to penetrate rat skin

Yuka Hiruta [a], Yoshiyuki Hattori [a], Kumi Kawano [a], Yasuko Obata [b], Yoshie Maitani [a,*]

[a] *Institute of Medicinal Chemistry, Hoshi University, Ebara 2-4-41, Shinagawa-ku, Tokyo 142-8501, Japan*
[b] *Department of Pharmaceutics, Hoshi University, Ebara 2-4-41, Shinagawa-ku, Tokyo 142-8501, Japan*

Received 18 January 2006; accepted 30 April 2006

Abstract

Beta-sitosterol 3-β-D-glucoside (Sit-G), an absorption enhancer, was incorporated into ultra-deformable vesicles containing bleomycin to attenuate drug toxicity in human keratinocytes. The presence of Sit-G increased drug entrapment and improved in vitro stability of ultra-deformable vesicles. Confocal laser scanning microscopy revealed the extent to which Sit-G facilitated the penetration of ultra-deformable vesicles containing fluorescent probes into rat skin upon non-occlusive topical application. Furthermore, treatment with preparations incorporating Sit-G resulted in elevated epidermal and dermal concentrations of bleomycin. Ultra-deformable formulation contained Sit-G maintained flexibility for penetration through the skin, increased entrapment efficiency of bleomycin and stability in vitro, and significantly increased distribution of bleomycin in epidermis and dermis compared with those without Sit-G.

Keywords: Ultra-deformable vesicle; Bleomycin; Skin permeation; Sodium cholate; Sterylglucoside

1. Introduction

The surface of human skin consists of the epidermis and stratum corneum (SC) layers. Despite their natural barrier properties, several drugs have successfully been delivered through these layers and the use of transdermal drug delivery systems have recently increased in popularity. In order to cross intact skin, drug carriers must either pass through corneocytes, or in between them via intercellular spaces. Many approaches have been developed to either destroy or fluidize the lipid bilayers, thereby, enhancing the penetration of drugs [1]. The diffusivity and solubility of the drug carrier in the SC and epidermis are critical parameters, which control the rate of drug permeation in skin [2].

Lipid vesicles drug delivery systems can be biocompatible in humans and incorporate both hydrophilic and lipophilic drugs [3]. Edge activators can increase the elasticity of bilayers formed from the redistribution of amphiphilic lipids [4] and such ultra-deformable vesicles have been shown to penetrate intact skin via transdermal osmotic gradients and hydration forces [5]. Examples of edge activators include the surfactants: sodium cholate, sodium deoxycholate [6,7], Tween 80 and Span 80 [8].

Bleomycin is an established anti-tumour drug used in the treatment of non-melanoma skin cancer (NMSC). Recent work has shown that bleomycin can be encapsulated in ultra-deformable liposomes [9] and this preparation may be useful for topical chemotherapy of NMSC [10].

Beta-sitosterol 3-β-D-glucoside (Sit-G, Fig. 1) exhibits slight solubility in water and oil. Particulate Sit-G exhibited the novel capability of promoting transport of peptide drugs through the intestinal and nasal mucosae by being ascribed to the glucose residue [11,12]. Sit-G was expected to be an absorption enhancer for skin.

The purpose of this investigation is to study the physical properties of ultra-deformable liposomes incorporating Sit-G.

* Corresponding author. Tel./fax: +81 3 5498 5048.
E-mail address: yoshie@hoshi.ac.jp (Y. Maitani).

0168-3659/$ - see front matter © 2006 Elsevier B.V. All rights reserved.
doi:10.1016/j.jconrel.2006.04.016

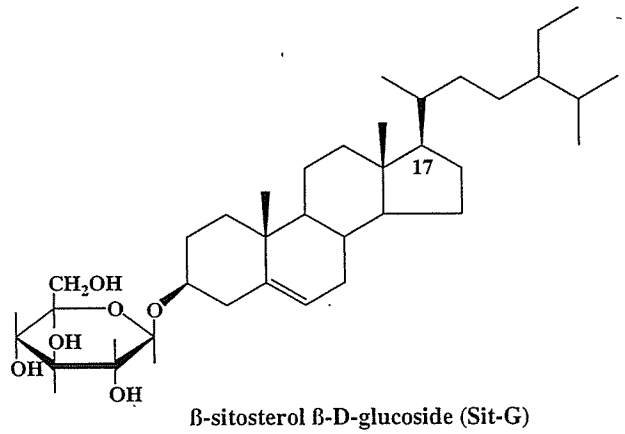

ß-sitosterol ß-D-glucoside (Sit-G)
MW; 580.60

Fig. 1. Chemical structure of β-sitosterol β-D-glucoside (Sit-G).

In order to enhance permeation of drugs through skin, we developed a novel formulation of ultra-deformable vesicles incorporating an absorption enhancer, Sit-G.

2. Materials and methods

2.1. Materials

Bleomycin hydrochloride for injection (BLM) was a gift from Nippon Kayaku Co. (Tokyo, Japan). Egg phosphatidylcholine (EPC) was purchased from NOF Corp. (Tokyo, Japan). Sit-G was obtained from Essential Sterolin Products (Midrand, South Africa). Tween 80 (Tween) and calcein were purchased from Tokyo Kasei Kogyo Co. Ltd. (Tokyo, Japan). Sodium cholate (Cholate), sodium perchlorate and urethane were obtained from Sigma Chemicals Co. (St. Louis, MO, U.S.A.). 1,1′-Dioctadecyl-3,3,3′,3′-tetramethylindocarbocyanine perchlorate (DiI) was purchased from Lambda Probes and Diagnostics (Graz, Austria). Other chemicals used were of reagent grade and purchased from Wako Pure Chemical Industries Ltd. (Osaka, Japan).

2.2. Preparation of ultra-deformable vesicles entrapped with calcein or BLM

Ultra-deformable vesicles were prepared by a dry film method. Briefly, lipid mixtures of EPC, Tween or Cholate, were dissolved in ethanol. Sit-G was dissolved in a chloroform/methanol solvent system at 2:1 v/v ratio. Then these lipid solutions were mixed. This organic solvent system was removed by rotary evaporation, under vacuum and at 55 °C. The dry lipid film was hydrated with either Milli-Q water, 1 mg/mL BLM aqueous solution, or 20 mM calcein solution, to yield empty vesicles, BLM-entrapped vesicles (BLM-vesicles), or calcein-entrapped vesicles, respectively. Vesicles labelled with DiI were prepared by addition of DiI (0.4 mol%) to lipid mixtures and hydrating with Milli-Q water. Vesicles were subsequently sonicated for 2–10 min using a bath-type sonicator (UT-205S, Sharp Corp., Osaka, Japan) at a 200 W energy output. Final total lipid concentration in all formulations was 10 mg/mL.

2.3. Vesicle size, morphology and ζ-potential measurements

Average diameters and ζ-potentials of vesicles were measured by dynamic light-scattering (DLS) and electrophoresis light-scattering methods, respectively (ELS 800, Otsuka Electronics, Osaka, Japan). All measurements were performed at 25±1 °C, after diluting the vesicle suspension with Milli-Q water.

Particle morphology was analyzed using a scanning electron microscope (SEM, JSM-5600LV, JEOL Ltd., Tokyo, Japan). Samples were coated with platinum prior to analysis. An accelerating potential of 15 keV was used and the images were obtained with a scintillating secondary electron detector.

2.4. Measurement of elasticity value

The elasticity value of bilayer of ultra-deformable vesicles was directly proportional to $J_{flux} \times (r_v/r_p)^2$;

$$\text{Elasticity} = J_{flux} \times (r_v/r_p)^2$$

where J_{flux} is the rate of penetration through a permeability barrier, r_v is the size of vesicles after extrusion and r_p is the pore size of the barrier [13,14]. To measure J, the vesicles were extruded through a polycarbonate membrane (Nuclepore, Whatman Inc., MA, USA) with a pore diameter of 50 nm (r_p), at a pressure of 0.5 MPa. After 5 min of extrusion, the extrudate was weighed (J), and the average vesicle diameter after extrusion (r_v) was measured by DLS.

2.5. Captured volume of ultra-deformable vesicles

Calcein-entrapped vesicles were separated from free (unentrapped) calcein by gel filtration chromatography using a Sephadex G-50 column and a mobile phase of 1/10 diluted phosphate-buffered saline (1/10 PBS). Vesicles were disrupted by addition of 10% (v/v) Triton X-100 (final concentration 0.1%) to release their calcein load. Entrapment efficiency was calculated by measurement of fluorescence emitted from entrapped calcein, and by EPC quantification via enzyme assay (Phospholipid B Test Wako, Wako Pure Chemical Industries Ltd.). Captured volume was obtained from calculated values of calcein entrapment efficiency and total post-filtration lipid concentration [15].

2.6. Determination of BLM-entrapment efficiency

Free BLM was separated from entrapped BLM using a Sephadex G-50 column and a mobile phase of 1/10 PBS. Unentrapped BLM was quantified by a UV-spectrophotometer (UV-1700 Phamaspec, Shimadzu Corp., Kyoto Japan) at 292 nm. Entrapment efficiency of BLM was calculated

indirectly from the amount of free drug, according to the following equation:

$$\text{Entrapment efficiency } (\%) = (1-B_f/B_t) \times 100$$

where B_f was the amount of free BLM and B_t was the total amount of BLM.

2.7. Physical stability study of BLM-vesicles in vitro

The stability of BLM-vesicles (10 mg/mL total lipid concentration) was evaluated by monitoring entrapment efficiency of BLM for 1 h at 37 °C [8]. Samples of the original vesicle suspensions, unfiltered and undiluted, were incubated at 37 °C. After 1 h, 100 μL aliquots were taken for determination of entrapment efficiency using the method in Section 2.6. Entrapment efficiency was calculated indirectly from the percentage of drug released. The amount entrapped at start time was normalized to 100%.

2.8. Animals

Wistar rats (male, 7 weeks, 190–220 g) and hairless rats (male, 7 weeks, 190–210 g) with clean status were purchased from Tokyo Laboratory Animal Science Co., Ltd. (Tokyo, Japan) and Sankyo Labo Service Corp. (Tokyo, Japan), respectively. They were housed in animal facilities under standard laboratory conditions prior to experimentation.

2.9. In vivo skin deposition and partitioning of BLM

Prior to experimentation, hair was carefully removed with an electric clipper from the abdominal area of Wistar rats under anesthesia (intra-peritoneal injection of urethane, 1 g/kg). Cevc and Blume [5] had previously recommended non-occlusive application for optimum transdermal drug delivery with ultra-deformable vesicles. The individual BLM-vesicle suspension containing 157 μg of liposomal BLM without gel filtration and the BLM solution (157 μg BLM using 1 mg/mL) were non-occlusively applied on the abdomen of rats (3.14 cm^2) for either 3 or 12 h. Rats were kept on their back on a heating pad during the sedation period. Blood sample (1 mL) was collected from the jugular vein periodically for either 3 or 12 h after dosing, and then centrifuged at 13,000 rpm for 4 min to obtain serum. After percutaneous administration of suspension, the residual suspension was removed from the skin surface with a cotton swab with warm water. The full-thickness skin was then separated from the underlying tissue. The serum and full-thickness skin was stored at −20 °C until HPLC analysis.

For in vivo skin partitioning of BLM after 12 h application, the BLM-vesicle suspensions remaining on the skin surface were wiped off with warm water. Stratum corneum (SC) was obtained using tape-strip technique. Ten strips and stripped skin (viable epidermis plus dermis) were further processed for HPLC analysis.

2.10. Sample preparation and HPLC assay

The serum (400 μL) was also centrifuged at 13,000 rpm for 4 min following to addition of 20% (w/v) trichloroacetic acid (TCA, 100 μL). The full-thickness and stripped skin were cut into small pieces and homogenized in 2 mL of 10 mM sodium perchlorate in 0.1% aqueous phosphoric acid (solvent A). After addition of 1 mL of 20% (w/v) TCA, the homogenate was centrifuged at 15,000 rpm for 5 min. The supernatants of serum and sample (300 μL) were directly injected into the HPLC system to determine the concentration of BLM. The recovery of added amounts of BLM to serum and skin homogenate was 89.6 ±9.6% and 87.9±16.7%, respectively. The SC tape-strips were soaked in 5 mL of solvent A for 5 h at room temperature. After removal of the tapes, SC sample was freeze-dried and dissolved in 800 μL of solvent A.

The HPLC analysis was performed at 25 °C. The system was consisted of SCL-10A system controller, LC-10AT liquid chromatograph, SIL-10AF auto injector, SPD-10A UV spectrophotometric detector at 240 nm (Shimadzu Corp.), and a C_{18} column (YMC-Pack, ODS-A A-302, 150×4.6 mm I.D., YMC Co., Ltd., Japan). The mobile phase was consisted of solvent A and acetonitrile (solvent B). A line gradient was applied from 5% to 25% solvent B for 20 min, increasing within 2 min to 100% B and hold for a 2 min and followed by post-time of 8 min under the initial condition [16]. The flow rate was set at 1 mL/min.

2.11. In vivo distribution of fluorescent-labeled ultra-deformable vesicles

Vesicle contained 16% (w/w) Cholate and 5% (w/w) Sit-G (CS-vesicles) suspension labeled by both DiI and calcein (551 μL; containing 14.8 mM of total lipid, 59 μM DiI and 20 mM calcein) without gel filtration, the mixture suspension of 20 mM calcein and DiI-labeled CS16-vesicles (Table 1) (551 μL; containing 14.8 mM of total lipid and 59 μM DiI) and the mixture solution (551 μL) of 20 mM calcein and 59 μM DiI were applied on the abdominal skins of hairless rats for 3 h

Table 1
The formulation of ultra-deformable vesicles

Vesicles	EPC	Tween 80 (T)	Sodium cholate (C)	Sit-G (S)
	% (w/w)			
EPC	100	–	–	–
T6	94	6	–	–
10	90	10	–	–
16	84	16	–	–
26	74	26	–	–
C6	94	–	6	–
10	90	–	10	–
16	84	–	16	–
26	74	–	26	–
CS6	89	–	6	5
10	85	–	10	5
16	79	–	16	5
26	69	–	26	5

T-, C- and CS-vesicle were composed of Tween 80, sodium cholate, and sodium cholate and Sit-G, respectively.

under anesthesia. After the removal of excess suspension, the skins administered were excised, washed three times with Milli-Q water and then dried with cotton swab. The skins were embedded in OCT compound (Tissue-Tek, Sakura Finetechnical Co., Ltd., Tokyo, Japan) and processed for frozen sectioning. The embedded skins were sectioned; frozen sections 20 μm apart of both cut surfaces. Each frozen section was mounted on a MAS coat slide glass (SUPERFROST®, Matsunami, Osaka, Japan), and examined microscopically. A confocal laser-scanning microscope (CLSM, Radiance 2100, Bio-Rad Laboratories, Inc., Hercules, CA, U.S.A.) was employed for imaging. For DiI, maximum excitation was performed by a 543-nm line of internal He–Neon laser, and fluorescence emission was observed with long pass barrier filter 560DCLP. Calcein was imaged using the 488 nm excitation line of an argon laser, and fluorescence emission was observed with a filter HQ515/30. The contrast level and brightness of the images were adjusted.

2.12. Statistical analysis

Significant differences in the mean values were evaluated by the Student's unpaired *t*-test. A *p*-value of less than 0.05 was considered to be significant.

3. Results

3.1. Elasticity of vesicles

Elasticity is an important feature of ultra-deformable vesicles that differentiates it from other lipid disperse systems which are typically non-elastic. Four formulations were used (Table 1): control vesicles containing only EPC (EPC-vesicles), EPC-vesicles containing a surfactant (Tween or Cholate, T- or C-vesicles), and C-vesicles incorporating 5% (w/w) Sit-G (CS-vesicles).

Average vesicle diameters of each preparation, before and after extrusion, are shown in Table 2. Preparations containing 26% (w/w) Cholate, either with (CS26) or without (C26) 5% (w/w) Sit-G, exhibited average vesicle diameters of 66 nm. Average vesicle diameters of all other preparations were in the range of 125–155 nm. Over the course of 5 months storage at room temperature, significant changes in vesicle size were only observed in the control preparation (data not shown). A reduction in average vesicle diameter was observed in all preparations after extrusion. Except for C26, CS26 and control formulations, the average vesicle diameter of ultra-deformable vesicles remained above 100 nm after extrusion (Table 2).

Table 2
Size of empty ultra-deformable vesicles before and after extrusion through polycarbonate membrane with a pore size of 50 nm

Vesicles	Size before extrusion (nm)	Size after extrusion (nm)
EPC	155.4±9.2	80.3±9.0
T6	150.7±13.3	102.7±17.2
10	139.6±5.3	114.7±1.0
16	136.7±7.8	102.3±10.4
26	125.4±7.9	112.6±12.8
C6	156.3±9.2	122.7±3.7
10	143.3±3.3	122.9±0.7
16	140.0±5.2	108.4±2.5
26	66.6±15.4	48.6±9.9
CS6	143.0±8.9	114.7±1.1
10	140.0±4.1	112.5±2.9
16	148.0±1.0	110.5±0.8
26	66.1±23.1	52.8±17.4

Values represented as mean±S.D.(n=3).

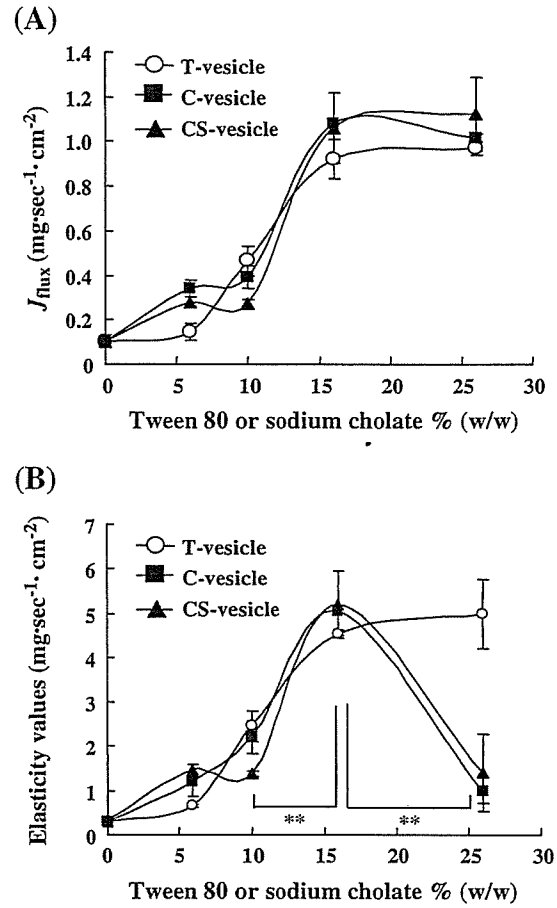

Fig. 2. J_{flux} (A) and calculated elasticity values, $J_{flux} \times (r_v/r_p)^2$ (B) of empty ultra-deformable vesicles in relation to the content of Tween 80 or sodium cholate. Each value represents the mean±S.D. (n=3). **p<0.01.

J_{flux} started at 16% (w/w) surfactant concentration in T-, C- and CS-vesicles (Fig. 2A) and elasticity of C- and CS-vesicles peaked to plateau at this concentration (Fig. 2B). At the highest concentrations of surfactant, reductions of vesicle size and elasticity were observed in C26 and CS26 (Table 2 and Fig. 2B), whereas no reduction of them was observed in T26. Elasticity of the preparations (T- or C-vesicles) in this investigation was comparable with published data [8].

The recovery of vesicle suspensions after extrusion was determined by measuring EPC concentrations in the extrudate when the passage of vesicles through pores much smaller than their own diameter (Fig. 3). The recovery of EPC of EPC-vesicle was approximately 10%. That in T-, C- and CS-vesicles was increased with an increase of surfactant

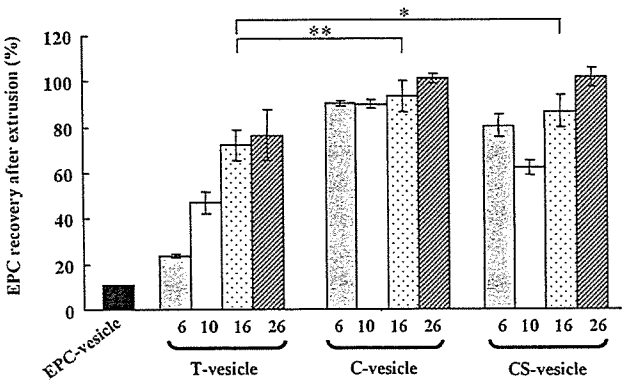

Fig. 3. EPC recovery (%) in vesicle suspensions after extrusion through polycarbonate membrane with a pore size of 50 nm. Each value represents the mean±S.D. (n=3). *p<0.05, **p<0.01.

content in each formulation. C16- and CS16-vesicles with maximum elasticity passed through the polycarbonate membrane showed about 80% of EPC, which was significantly higher compared with that of T-vesicles (p<0.05). C26- and CS26-vesicles showed high EPC recovery because of small sizes.

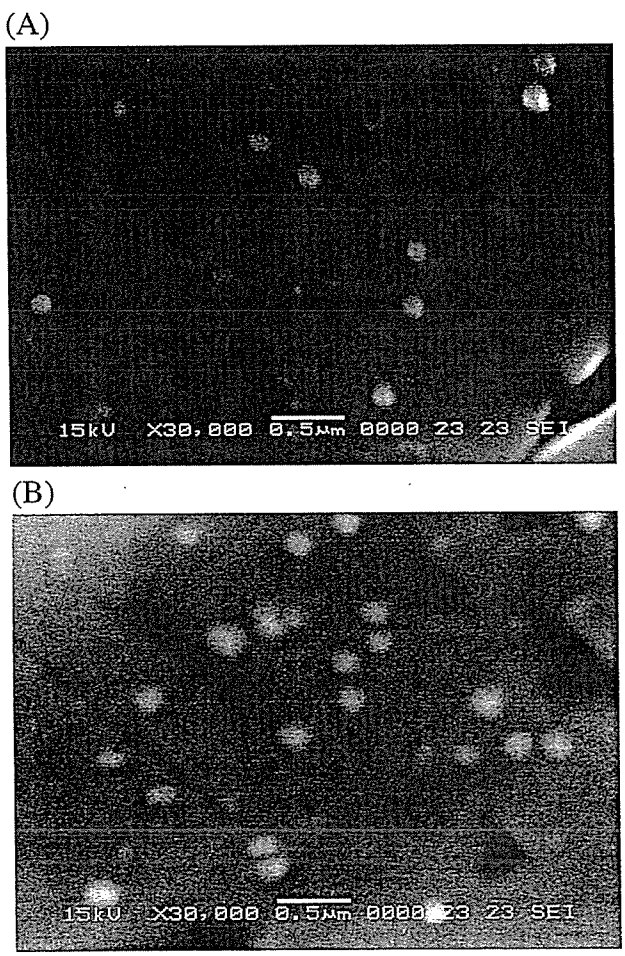

Fig. 4. Scanning electron micrographs of C16-vesicles before (A) and after extrusion (B) through a polycarbonate membrane with a pore size of 50 nm. Scale bar=0.5 μm.

The morphology of vesicles was also investigated by scanning electron microscopy. C16-vesicles were chosen for SEM observation because of their high elasticity and EPC recovery. C16-vesicles after extrusion appeared as particles with a diameter of above 100 nm, like vesicles before extrusion (Fig. 4A, B). High recovery of EPC and SEM observation of vesicle suspensions after extrusion suggest that high elasticity of the bilayers, ultra-deformable vesicles might squeeze themselves and pass through pores much smaller than their own diameter.

3.2. Captured volume and ζ-potential of empty vesicles and characterization of BLM-entrapped vesicles

Based on the result of extrusion measurement, highly elastic T16-, C16- and CS16-vesicles were chosen as the formulations of BLM-vesicles (T16-, C16- and CS16-BLM, respectively) for stability study. The volume of entrapped aqueous fluid per mole of lipid represented the captured volume afforded by the preparation, and this parameter has been linked with many membrane properties [17,18]. In this experiment, captured volume was calculated from the entrapment efficiency of calcein. Captured volume of the T16-, C16- and CS16-vesicles was 1.7±0.06 μL/μmol, 1.4±0.11 μL/μmol and 1.0±0.03 μL/μmol, respectively (Table 3). This finding suggests that the inner aqueous phase of vesicles was significantly decreased with the increase of other components into EPC.

C16- and CS16-vesicles were more negatively-charged than T16-vesicles (Table 3). Vesicles containing Cholate showed particularly negative ζ-potentials, but CS16-vesicles showed less negative ζ-potential than C16-vesicles, suggesting that Sit-G might disturb the charge of Cholate at the surface of vesicles. The entrapment efficiencies of BLM-vesicles are given in Table 3. The average size of BLM-vesicles was about 145–158 nm. Of the formulations, higher efficiency of BLM was as follows; CS16-BLM>C16-BLM>T16-BLM≈EPC-BLM, and CS16-BLM gave the highest entrapment efficiency; 28.5%. C16 was more negative than CS16, but had lower efficiency. This finding suggests that positively-charged BLM might lead to the

Table 3
Characteristics of empty and BLM-vesicles

Vesicles	Empty vesicles		BLM-vesicles[a]
	Captured volume[b] (μl/μmol)	ζ-potential (mV)	Entrapment efficiency (%)
EPC			10.4 ± 0.8
T16	1.7 ± 0.06	−3.48	13.2 ± 2.1
C16	1.4 ± 0.11	−37.6	22.7 ± 1.1
CS16	1.0 ± 0.03	−30.7	28.5 ± 1.7

Each value represents the mean±S.D.(n=3) except ζ-potential (n=2). *p<0.05.
[a]Average size of BLM-vesicles was 145–158 nm.
[b]Ratio of captured volume (μL) over mole (μmol) of lipids. Captures volume was calculated from entrapment efficiency of calcein.

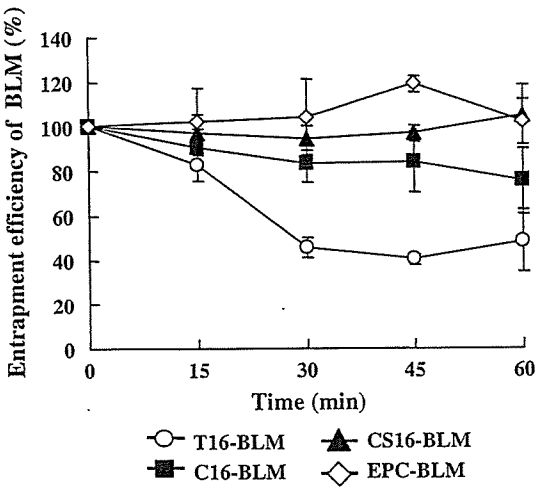

Fig. 5. Stability of BLM-vesicles by monitoring entrapment efficiency. BLM-vesicles prepared using 1 mg/mL BLM aqueous solution without gel filtration were incubated at 37 °C. Each value represents the mean±S.D. (n=3). Total lipid concentration of each vesicle was 10 mg/mL.

binding with Cholate and also interact with Sit-G molecules incorporated into the membrane.

Fig. 5 illustrates the result of the stability of BLM-vesicles without gel filtration, assuming the entrapped amount to be 100% before incubation. Entrapment efficiency of CS16-, C16- and EPC-BLM preparations after 1 h of incubation at 37 °C was approximately 105%, 80%, and 102%, respectively. Preparations made from CS16-BLM were very stable and similar to EPC-BLM, whereas T16-BLM showed rapid release of BLM such that over 50% of entrapped BLM was lost within the initial 30 min (Fig. 5). These differences might be due to variations in molecular ordering caused by using particular surfactants. Preparations made from CS16-BLM were stable and showed high BLM entrapment efficiency, suggesting strong interaction between BLM and the Sit-G incorporated in vesicle bilayers. After gel filtration, the entrapment efficiency of CS16-, C16- and EPC-BLM preparations were less than that without gel filtration after 1 h incubation at 37 °C (data not shown). This finding suggests that BLM was highly released from CS16-, C16- and EPC-BLM preparations after gel filtration at 37 °C. Consequently, in the following in vivo permeation studies, BLM-vesicles were used without gel filtration.

3.3. In vivo skin permeation and deposition of BLM

Skin permeation of BLM arising from preparations of C16-, CS16-, and EPC-BLM was examined in vivo. Free BLM aqueous solution (BLM sol.) was used as a control. The permeation profile of BLM as a function of time is presented in Fig. 6. The skin permeation of C16-, CS16-, and EPC-BLM showed 1.8±0.5, 3.1±0.4 and 0.8±0.2 dose% at 3 h and 4.0±1.0, 6.0±1.2 and 1.1±0.4 dose% at 12 h, respectively.

Skin permeation and deposition of BLM sol. showed no detectable levels of BLM, either in serum or in full-thickness skin (skin; <0.5 dose%, serum; <2.9 dose%). This indicated that free BLM did not permeate into the rat skin over a period of 12 h. The absorption of BLM into the skin from vesicle formulations was observed but serum concentrations of BLM were not detectable. Preparations of CS16-BLM showed significantly higher concentrations of BLM than EPC-BLM, at both 3 and 12 h (p<0.01).

Distribution of BLM in skin 12 h after application (Fig. 7) revealed that EPC-BLM preparations only showed detectable levels of BLM in SC and not beyond. By comparison, C16- and CS16-BLM showed preferential absorption of BLM into epidermis and dermis rather than merely residing in the SC. Preparations of CS16-BLM delivered higher skin concentrations of BLM than C16-BLM (p<0.01), and BLM levels in epidermis plus dermis were approximately twice as high as that

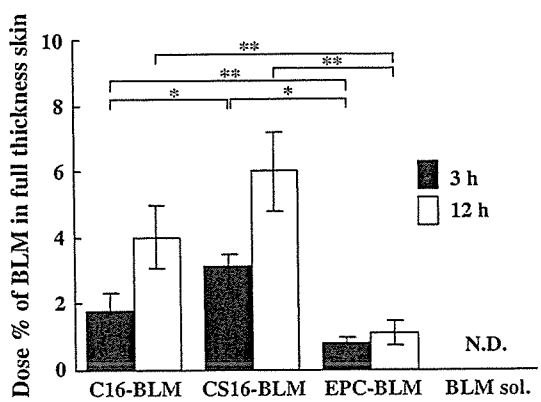

Fig. 6. Deposition of BLM in full-thickness skin 3 h and 12 h after application of ultra-deformable vesicles on Wistar rat. BLM-vesicles contained 157 μg of BLM as an entrapped amount without gel filtration, and the BLM solution (157 μg BLM using 1 mg/mL) were non-occlusively applied on the abdomen of rats (3.14 cm^2). N.D.; not detected. Each value represents the mean±S.D. (n=3), * p<0.05, ** p<0.01.

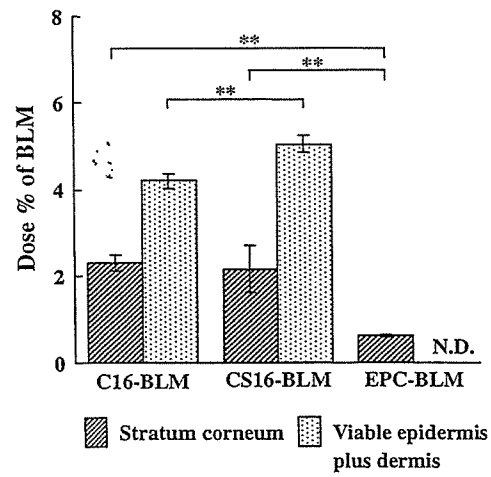

Fig. 7. Distribution of BLM in different layers of the skin of Wistar rat 12 h after non-occlusive application of vesicles. Vesicles contained 157 μg of BLM as an entrapped amount without gel filtration. Stratum corneum and viable epidermis plus dermis were obtained from the treated full-thickness skin. N.D.; not detected in viable epidermis plus dermis. Each value represents the mean±S.D. (n=3), ** p<0.01.